Some aspects of ocean heat transport by the shallow, intermediate and deep overturning circulations

Lynne D. Talley

Scripps Institution of Oceanography, UCSD, La Jolla, CA

The ocean's overturning circulation can be divided into contributions from: (1) shallow overturning in the subtropical gyres to the base of thermocline, (2) overturning into the intermediate depth layer (500 to 2000 meters) in the North Atlantic, North Pacific and area around Drake Passage, and (3) overturning into the deep layer in the North Atlantic (Nordic Seas overflows) and around Antarctica. The associated water mass structures are briefly reviewed including presentation of a global map of proxy mixed layer depth. Based on the estimated temperature difference between the warm source and colder newly-formed intermediate waters, and the formation rate for each water mass, the net heat transport associated with all intermediate water formation is estimated at 1.0-1.2 PetaWatts (1 PW = 10^{15} W), which is equivalent in size to that for deep water formation, 0.6-0.8 PW. The heat transport due to shallow overturn, calculated as the residual between published direct estimates of heat transport across subtropical latitudes and these heuristic estimates of the intermediate and deep overturning components, is about 0.5 PW northward for the North Pacific and North Atlantic subtropical gyres and 0.0 to 0.2 PW southward for each of the three southern hemisphere subtropical gyres, exclusive of the shallow overturn in the southern hemisphere gyres which is associated with Antarctic Intermediate Water and Southeast Indian Subantarctic Mode Water formation.

Direct estimates of meridional heat transport of 1.18 PW (North Atlantic) and 0.63 PW (North Pacific) at 24°N are calculated from *Reid's* [1994, 1997] geostrophic velocity analyses and are similar to previously published estimates using other methods. The new direct estimates are decomposed into portions associated with shallow, intermediate and deep overturn, confirming the heuristic estimate for the North Pacific, where the shallow gyre overturning heat transport accounts for about 75% of the total and intermediate water formation for the remainder. The direct estimate for the North Atlantic indicates the opposite - about 75% of the total heat transport is associated with intermediate and deep water formation, split approximately

Mechanisms of Global Climate Change at Millennial Time Scales
Geophysical Monograph 112

equally, with the remainder associated with the shallow gyre overturn. the difference from the heuristic estimate for the North Atlantic suggests that the source waters for the intermediate and deep water overturn originate within the Gulf Stream at an average temperature warmer than 14°C.

1. INTRODUCTION

Meridional heat transport in the ocean is associated with heat gain and loss at the sea surface and hence transformation of surface water properties. The ocean and atmosphere together transport approximately 5-6 PW (1 PW = 1 PetaWatt = $10^{15}W$) of heat poleward in each hemisphere on an annual average; of this, approximately one-third to one-half is carried by the oceans [*Oort and Von der Haar,* 1976; *Talley,* 1984; *Hsiung,* 1985; *Keith,* 1995; *Josey et al.,* 1996]. The distribution of meridional ocean heat transport depends on ocean basin and the distribution of water mass transformation. The major elements of the net transfer of heat from the ocean to the atmosphere include heating throughout the tropics and large heat loss in the Gulf Stream and Kuroshio where warm northward boundary currents meet cold, dry continental air [Figure 1 after *Hsiung,* 1985]. [For recent maps, with similar patterns, see *da Silva et al.,* 1994; *Barnier et al.,* 1995; *Josey et al.,* 1997.] An asymmetry between the North Atlantic and North Pacific is evident in the large areas of heat loss extending up into the Nordic Seas in the North Atlantic. In the southern hemisphere, the more recent maps which extend to Antarctica show regions of heat loss in the poleward western boundary currents, with lower amplitudes than in the Kuroshio and Gulf Stream. In all versions of air-sea heat flux, large heat loss is not observed in the primary formation regions of most intermediate and deep water masses (described below). The absence of high surface flux may reflect a fair weather bias in data coverage but more likely is an indication that buoyancy loss associated with these water mass transformations is a gradual, broad-scale, cumulative process, culminating in a geographically-limited formation of the denser water.

Superimposed on Figure 1 are various published direct estimates of ocean heat transport at subtropical latitudes based on *in situ* temperature measurements and velocity estimates. All basins, except the South Atlantic, transport heat poleward across their subtropical gyres. The South Atlantic transports heat equatorward to the North Atlantic, feeding the northern hemisphere deep water formation.

Because ocean heat transport is linked to water mass transformation, it is useful to estimate the relative contribution of each of the types of water mass transformation to the overall heat transport. *Speer and Tziperman* [1992] and *Speer* [1992] related surface heat fluxes to water mass formation in isopycnal outcrop regions and were able to identify some especially marked transformations, particularly those associated with Subtropical and Subpolar Mode Waters at midlatitudes. Deep and intermediate water formation are not easily captured using Speer and Tziperman's method due to the localized and in some cases, subsurface, processes involved.

In situ temperature measurements and direct velocity estimates, where available for the full water column, can be used to estimate the relative contribution of different water mass formations to the heat transport. For the North Atlantic and North Pacific respectively, *Hall and Bryden* [1982] and *Bryden et al.* [1991] decomposed the direct heat transport into a portion carried by the Ekman transport, the total baroclinic contribution (overall overturn), and a horizontal circulation (due to the temperature difference in northward and southward flows at the same depth). They also considered the contribution to the net heat transport of different parts of the gyre and water column. Hall and Bryden concluded that in the North Atlantic at 24°N almost all of the heat transport is carried by the conversion of warm northward-flowing waters into deep/intermediate waters. *Roemmich and Wunsch* [1985] came to the same conclusion using a 1980 reoccupation of the 1957 section used by Hall and Bryden. In contrast, for the North Pacific at 24°N, *Bryden et al.* [1991] showed that about half of the heat transport is due to shallow overturn in the subtropical gyre and the other half is due to intermediate water formation.

Roemmich and Wunsch [1985] (North Atlantic), *Rintoul* [1991] (South Atlantic), *Roemmich and McCallister* [1989] (North Pacific), *Wunsch et al.* [1983] (South Pacific) and *Toole and Warren* [1993]/*Robbins and Toole* [1997] (Indian) presented total mass transport in isopycnal, isothermal or constant pressure layers along zonal sections which completely cross the ocean basins at 24°N and 30°S. These presentations clearly show the distribution of net northward and southward flow as a function of depth and hence depict overturn (upwelling and downwelling).

In section 2, the principal water masses involved in the overturning are described, including the apparent

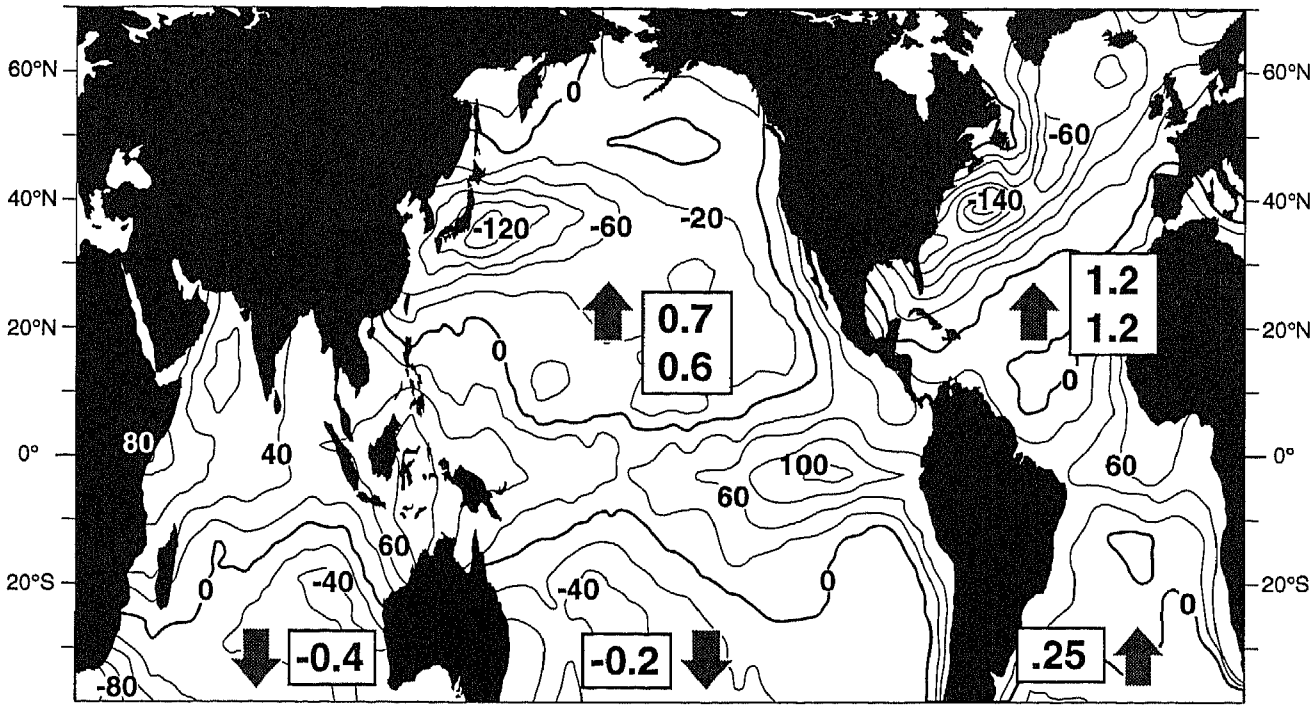

Figure 1. Ocean net heat gain (Wm^{-2}) after *Hsiung* [1985]. Positive numbers indicate heat gained by the ocean from the atmosphere. Direct estimates and directions of meridional heat transport are indicated for each subtropical gyre. The upper number in each box is from: North Pacific - *Bryden et al.* [1991]; North Atlantic - *Hall and Bryden* [1983]; Indian - *Robbins and Toole* [1997], including Indonesian throughflow; South Pacific - *Wunsch et al.* [1983]; South Atlantic - *Rintoul* [1991]. The lower number in the northern hemisphere boxes is calculated herein (section 3.2) using *Reid's* [1994, 1998] velocities and standard calculations for the Ekman layer transport.

precursors to the new water masses. Table 1 lists the acronyms used for water mass names. In section 3.1, heat transports associated with formation of each intermediate and deep water mass are estimated based on their formation rates and temperature change from their source waters. In section 3.2, *Reid's* [1994, 1997] velocity analyses at 24°N in the Pacific and Atlantic are used to calculate the heat transport due to shallow, intermediate and deep overturn. The net heat transports using Reid's velocities are comparable to those shown in Figure 1. The heuristic estimates of section 3.1 are then compared with the direct estimates of section 3.2, for the northern hemisphere only.

2. MAJOR OVERTURNING COMPONENTS: REVIEW OF WATER MASS DISTRIBUTIONS

Water mass formation can be thought of primarily as the densifying branch (downwelling) part of the large-scale overturn. Two processes dominate: open ocean buoyancy loss leading to mixed layer deepening, densification and convection (subtropical and subpolar mode water formation, Labrador and Greenland Sea intermediate water formation, Antarctic Intermediate Water formation), and buoyancy loss due to brine rejection under ice formation (North Pacific Intermediate Water formation, Antarctic Bottom Water formation, and possibly some aspects of Greenland Sea intermediate water formation). Upwelling and diffusion alter water mass properties and can be volumetrically significant even for narrowly-defined water masses such as the North Atlantic Deep Water where Antarctic Bottom Water upwells into it.

2.1. Winter Mixed Layer Depth

Water mass formation due to open ocean surface buoyancy loss is not a local process since mixed layer properties are cumulative along a flow path. Winter mixed layer depth is a useful indicator of vigorous surface layer processes and preconditioning for overturn. For the North Pacific, *Reid* [1982] showed that a useful

Table 1. Acronyms Used in the Text

Acronym	Text
AABW	Antarctic Bottom Water
AAIW	Antarctic Intermediate Water
LCDW	Lower Circumpolar Deep Water
LSW	Labrador Sea Water
NADW	North Atlantic Deep Water
NPIW	North Pacific Intermediate Water
PDW	Pacific Deep Water
SAMW	Subantarctic Mode Water
SEISAMW	Southeast Indian Subantarctic Mode Water
SPMW	Subpolar Mode Water
STMW	Subtropical Mode Water
WOCE	World Ocean Circulation Experiment

proxy for winter mixed layer depth is oxygen saturation. In the subtropical gyre Reid showed that the seasonal surface layer is generally supersaturated and that the 100% oxygen saturation horizon is a reasonable indicator of winter mixed layer depth. Because the winter surface layer in the subpolar region is undersaturated due to vigorous overturn, Reid found that the 94% saturation depth was a more useful proxy in the North Pacific's subpolar gyre.

In lieu of a complete analysis of the correspondence in each basin between oxygen saturation and winter mixed layer depth, the 95% oxygen saturation depth is used here (Plate 1). A global hydrographic data set comprised of all discrete bottle stations available from the one-time survey of the World Ocean Circulation Experiment (WOCE) hydrographic program and high quality hydrographic data from the National Oceanographic Data Center selected by J. Reid and A. Mantyla (personal communication) were used. Oxygen profiles were interpolated to 10 meter depths using an Akima cubic spline; the 95% saturation depth was then found through linear interpolation.

The deepest winter mixed layers, as indicated by depth of the 95% oxygen saturation, are close to and north of the Antarctic Circumpolar Current and are in the northern North Atlantic. The deep Southern hemisphere mixed layers are referred to as Subantarctic Mode Water [*McCartney,* 1977] and are the major precursor to Antarctic Intermediate Water formation. The Subantarctic Mode Waters (SAMW) are thickest in the southeast Indian Ocean and across the South Pacific. The easternmost SAMW in the Indian Ocean is the densest outcropping water in the combined South Atlantic and Indian subtropical gyre. The easternmost SAMW in the South Pacific is the densest outcropping water in the South Pacific's subtropical gyre and is the source of Antarctic Intermediate Water [*McCartney,* 1977].

The thick subpolar North Atlantic layers are referred to as Subpolar Mode Water (SPMW) [*McCartney and Talley,* 1982]. SPMW is a primary input to Labrador Sea Water and Greenland Sea Water and hence to intermediate and deep water formation in the North Atlantic.

Two important regions of intermediate/deep water formation do not have a deep mixed layer signature: the Okhotsk Sea (North Pacific Intermediate Water) and the Weddell/Ross Seas and Adelie Land (Antarctic Bottom Water). In these regions sea ice formation is the dominant process for buoyancy loss and is accompanied by production of a highly stratified, saline layer on the continental shelf which enters the deeper sea as a plume.

Within the western parts of the subtropical gyres are found locally thicker mixed layers. These are the Subtropical Mode Water formation sites and are an important component of the shallow overturn [*Speer and Tziperman,* 1992], although not the densest part of it. In the next set of subsections, the upper ocean, intermediate depth and abyssal overturning water masses are described briefly.

2.2. Upper Ocean - Subtropical Gyres

Shallow subtropical overturning has several components: poleward flow of warm water in the western boundary current, major buoyancy loss associated with formation and spreading of Subtropical Mode Water, and continued buoyancy loss leading to denser surface waters in the poleward, eastern gyre region, followed by a split into equatorward subduction beneath less dense waters and poleward flow into the subpolar regions. The subtropical circulations with their poleward western boundary currents and equatorward interior flows are indicated very schematically in Figure 2.

The thick layers of relatively homogenized water in the poleward-western corners of the subtropical gyres, adjacent to the poleward western boundary currents and their eastward, separated extensions (medium shaded regions in Figure 2) are the Subtropical Mode Waters (STMW). In the North Atlantic and North Pacific, STMW is associated with the largest surface buoyancy loss (Figure 1). Because the vertical stratification in the upper ocean in the North Atlantic is considerably weaker than in the North Pacific, the North Atlantic STMW is thicker and deeper. The southern hemi-

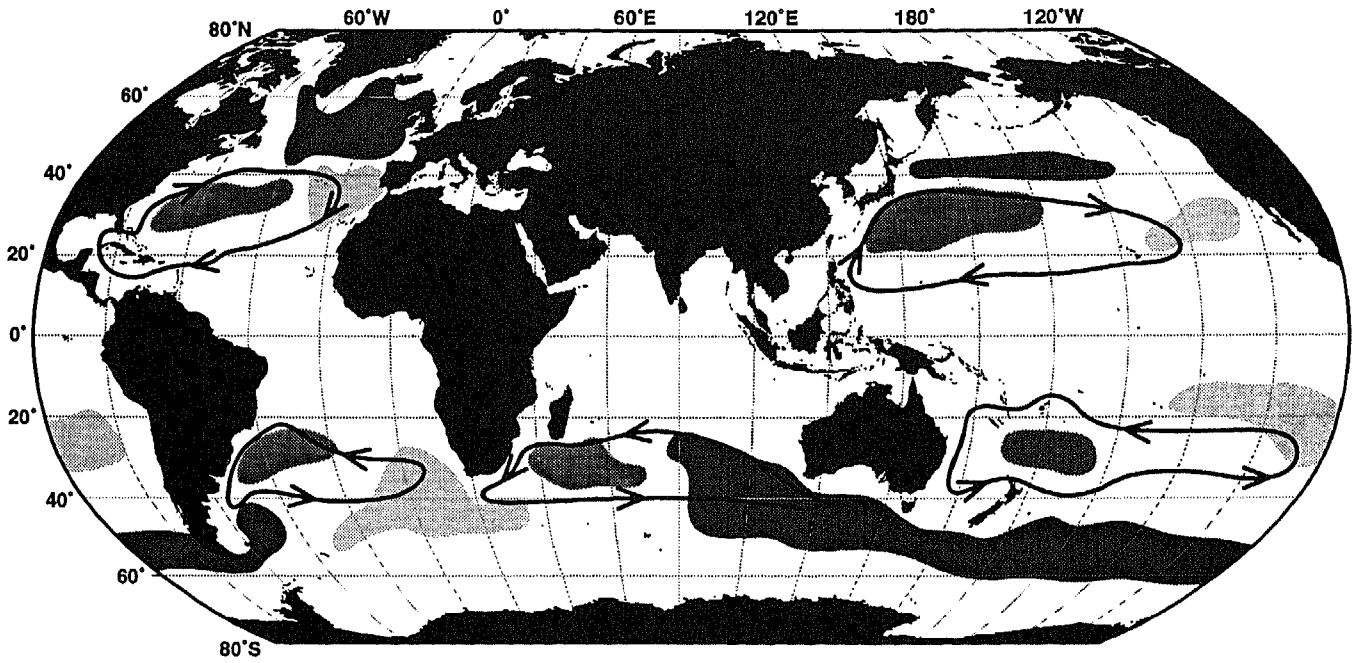

Figure 2. Subtropical mode water locations (medium shading). Low density mode waters of the eastern subtropical gyres (light shading). Highest density mode waters which subduct into the subtropical gyres (dark shading): Subpolar Mode Water in the North Atlantic, North Pacific Central Mode Water, and Subantarctic Mode Water in the southern hemisphere. Cartoons of subtropical gyre circulations are superimposed.

sphere STMW's, which are the group of thicker layers near 30°S, east of Brazil [*Tsuchiya et al.,* 1994], east of Madagascar [*Gordon et al.,* 1987; *Toole and Warren,* 1993] and north of New Zealand [*Roemmich and Cornuelle,* 1992], are somewhat less remarkable in thickness.

Warm, thick surface layers (light shading in Figure 2 and Plate 1) are also found on the eastern sides of each of the subtropical gyres. These layers are associated with low density mode waters which have not been as completely described as other mode waters. These low density mode waters are at 20 - 30° latitude in the North Pacific [*Hautala et al.,* 1998], the Madeira Mode Water in the North Atlantic [*Käse et al.,* 1985], and mode waters in the South Atlantic, Indian and South Pacific at 20 - 40°S. These thick mixed layers are not associated with particularly large local buoyancy loss (Figure 1). All are subducted equatorward in their respective gyres.

The densest surface waters in each subtropical gyre are found at the poleward, eastern boundary. These also are relatively thick "mode waters" (dark shading in Figure 2). When subducted equatorward, they form the bottom of the directly ventilated subtropical thermocline. There is nothing remarkable about the surface buoyancy loss (Figure 1) in the area where these poleward, eastern mode waters are found. Rather they appear to be a dynamical feature of the gyre with perhaps a slight enhancement due to surface buoyancy loss. These poleward, eastern mode waters are: the southern portion of the Subpolar Mode Water in the North Atlantic [*McCartney and Talley,* 1982], the North Pacific Central Mode Water [*Suga et al.,* 1997], the southeast Indian Subantarctic Mode Water [*McCartney,* 1977, 1982], and the southeast Pacific Subantarctic Mode Water or Antarctic Intermediate Water [*McCartney,* 1977, 1982].

In section 3.2 below, the maximum vertical extent of the shallow overturning is taken to be the maximum subtropical gyre surface density in winter and includes all of the subtropical mode waters. The poleward edge of the subtropical gyre is given by the zero of the annual average Sverdrup transport streamfunction. The nominal maximum potential densities relative to the sea surface in the North Pacific and North Atlantic are $\sigma_\theta = 26.2$ and 27.3, respectively [see *Yuan and Talley,* 1992 and *McCartney,* 1982, respectively]. In the southern hemisphere, the subtropical circulations are divided here at New Zealand where the eastward flow of the Antarctic Circumpolar Current is especially constricted. The maximum potential density of

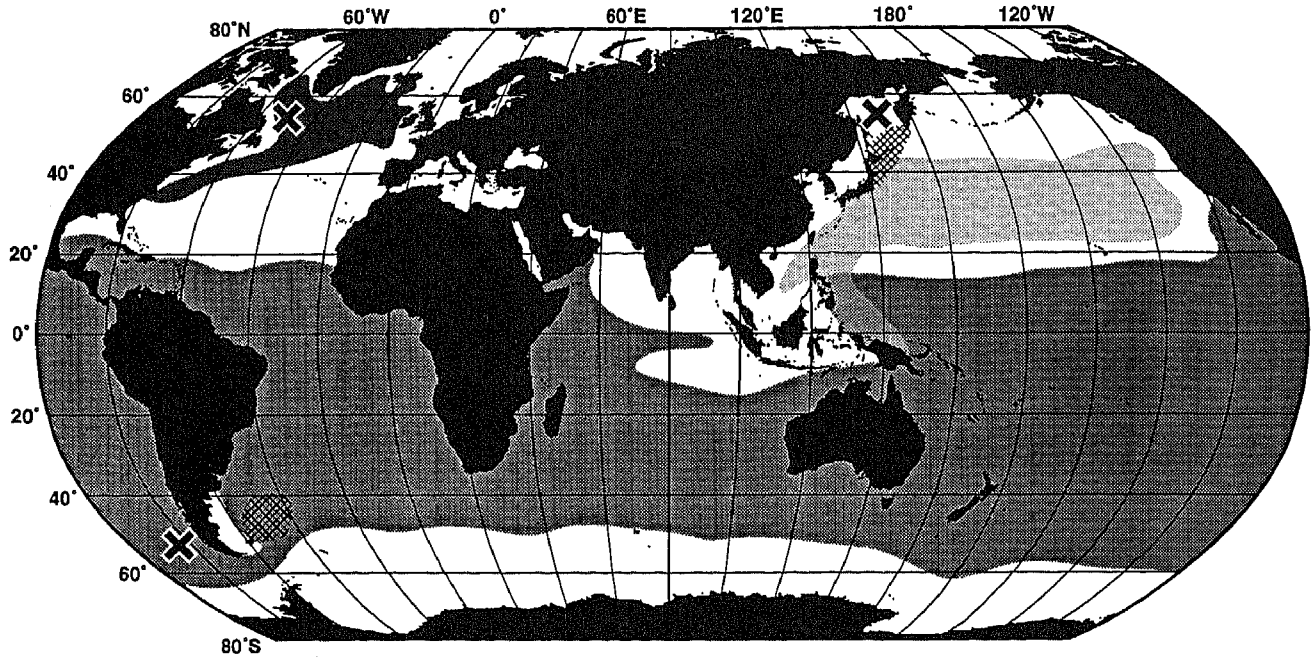

Figure 3. Locations of the intermediate water salinity minima Labrador Sea Water (LSW) (dark) [*Talley and McCartney,* 1982], North Pacific Intermediate Water (NPIW) (light) [*Talley,* 1993], and Antarctic Intermediate Water (AAIW) (medium) [*Talley,* 1998]. The total geographic influence of the newly-renewed intermediate waters extends well beyond these salinity minimum regions. (For instance, renewed water NPIW fills the North Pacific's subpolar gyre, but is not a salinity minimum due to the lower salinity surface waters [*Talley,* 1993]; the high oxygen signature of LSW extends into the South Atlantic as Middle North Atlantic Deep Water [*Wüst,* 1935]; high silica associated with AAIW extends to the subpolar North Atlantic [*Tsuchiya,* 1989].) Primary formation areas for the intermediate waters are indicated with X's. Hatching indicates regions where mixing is essential for setting properties of the intermediate waters near their sources. (Clearly mixing occurs globally throughout the water mass extent, causing gradual changes in properties and erosion of vertical property extrema.) The NPIW and AAIW salinity minima overlap in the western tropical Pacific.

the combined South Atlantic/Indian subtropical gyre is $\sigma_\theta = 26.8$ to 26.9, corresponding to the southeast Indian SAMW (SEISAMW) found south of Australia (see below). The maximum potential density of the South Pacific subtropical gyre is about $\sigma_\theta = 27.1$, corresponding to SAMW of the southeast Pacific, which is identical with Antarctic Intermediate Water (AAIW) there. Thus formally speaking AAIW in the South Pacific is the densest shallow overturning water mass.

2.3. Intermediate Water Formation

The intermediate layer of a given subtropical and tropical ocean can be defined to lie between the maximum subducted density in the subtropical gyre and the deep water described in the next subsection, that is, from about 500 to 2000 meters depth, depending on basin and location. The sources of intermediate waters result in salinity signatures. The fresh intermediate waters (Figure 3), originating from freshened surface subpolar waters, are the Labrador Sea Water (LSW), North Pacific Intermediate Water (NPIW), and Antarctic Intermediate Water (AAIW). Saline intermediate waters are formed in the Mediterranean and Red Seas but are not considered in section 3 since their total formation rate, temperature change and overturning heat transport are low.

The fresh intermediate waters are injected to intermediate depth at specific locations indicated in Figure 3. The water masses are: the Labrador Sea for the LSW [*Lazier,* 1980; *Clarke and Gascard,* 1983; *Talley and McCartney,* 1982], the Okhotsk Sea for the NPIW [*Talley,* 1991, 1993], and the region around southern South America for AAIW [*McCartney,* 1977; *Talley,* 1996a].

Each of the fresh intermediate waters is formed in a different manner. LSW is formed by intermediate depth

convection, to about 1500 m, acting on the thick surface layer of Subpolar Mode Water (Plate 1 and dark shading in Figure 2) whose density and thickness increase as it circulates cyclonically around the subpolar gyre [*McCartney and Talley,* 1982]. NPIW forms through brine rejection during sea ice formation in the northwestern Okhotsk Sea [*Kitani,* 1973; *Talley,* 1991], followed by strong tidal mixing [*Talley,* 1991], and possibly including deep convection in the southern Okhotsk Sea [*Wakatsuchi and Martin,* 1990; *Freeland et al.,* 1998]. NPIW enters the subtropical gyre in the North Pacific through strong interaction between the Oyashio and Kuroshio [*Talley,* 1993; *Talley et al.,* 1995]. AAIW in the South Pacific is the densest Subantarctic Mode Water (thick layers off Chile in Plate 1 and dark shading in Figure 2) and is subducted northward into the subtropical gyre [*McCartney,* 1977; *Talley,* 1996a]. Pacific AAIW is thus actually part of the shallow overturn. AAIW in the Atlantic and Indian Oceans derives from advection of the southeast Pacific AAIW through Drake Passage with additional modification in that region. AAIW enters the Atlantic's subtropical gyre through strong interactions between the Falkland and Brazil Currents [*Talley,* 1996a].

The total extent of the subpolar-origin intermediate water is of course much greater than depicted in Figure 3, which shows only the locations of the actual salinity minima. Although the salinity extrema erode away beyond these regions, a significant amount of the water at the intermediate densities nevertheless has originated in the intermediate water formation sites. For instance the influence of AAIW in the North Atlantic has been tracked through a high silica signal [*Tsuchiya,* 1989], and the influence of LSW in the South Atlantic is evident as an oxygen maximum [Middle North Atlantic Deep Water in *Wüst,* 1935].

The primary source waters of the fresh intermediate waters within their gyre regions are the surface waters in the southwestern regions of the northern hemisphere subpolar gyres (for NPIW and LSW) and the surface waters east of the Falkland/Brazil confluence for the AAIW [*McCartney,* 1977]. The source water temperatures are taken to be 12°to 15°C (Table 2, used in section 3.1).

2.4. Deep Water Formation

Deep water lies below about 2000 meters. There are two surface sources for the deep waters of the main ocean basins: (1) the intermediate waters of the Nordic Seas [*Swift et al.,* 1980] which overflow into the North Atlantic producing the densest part of the North Atlantic Deep Water (NADW), and (2) dense water formed around Antarctica, primarily in the Weddell and Ross Seas and along Adelie Land [*Rintoul,* 1998], producing bottom/deep waters known variously as Antarctic Bottom Water (AABW) or Lower Circumpolar Deep Water (LCDW).

In the North Atlantic, Nordic Sea overflow water is joined by the intermediate-depth, outflowing Labrador and Mediterranean Sea Waters, amalgamated into a single low nutrient, high oxygen water mass by the time of passage into the subtropical South Atlantic [*Wüst,* 1935]. The global influence of the high salinity NADW was demonstrated by *Reid and Lynn* [1971].

Various authors have shown that the temperature of the northward-flowing water in the South Atlantic that feeds NADW formation must be at least 12°C [*Gordon,* 1986; review in *Talley,* 1996b]. A temperature of 14°C is used herein, which is the winter surface water temperature in the North Atlantic Current region, assuming that this water is the principal warm water source of NADW [*McCartney and Talley,* 1984].

The southern hemisphere deep and bottom waters are primarily formed through ice processes on the shelves. The densest of these waters do not stray far from the Antarctic basins, confined by topography. The "Antarctic Bottom Water" observed at mid-latitudes originates at shallow to intermediate levels south of the Antarctic Circumpolar Current [e.g., *Reid,* 1994]. A rough depiction of the influence of AABW is shown in Figure 4 based on the location of waters at $\sigma_4 = 45.92$ kg/m^3. At this potential density relative to 4000 dbar, water of Nordic Sea origin is confined north of Newfoundland (light shading in Figure 4), separated from water of Antarctic origin (medium shading). At slightly lower potential densities (e.g. $\sigma_4 = 45.91$ kg/m^3), water from the two sources merge, and so although there is Antarctic influence, it is confounded with Nordic Sea influence.

The warm water source of Antarctic Bottom Water is most likely NADW that passes southward through the fronts of the Antarctic Circumpolar Current in the eastern South Atlantic and Indian Oceans. NADW upwells south of the Antarctic Circumpolar Current to supply most of the upper layer that is modified to produce AABW. Therefore the NADW temperature is chosen in section 3.1 for the source of AABW (Table 2).

3. HEAT TRANSPORTS AND WATER MASSES

Net heat transport is a useful concept when the mass balance is closed, hence reflecting the temper-

Table 2. Heuristic Heat Transports for Deep and Intermediate Waters

	Temperature change	Volume Transport	Heat Transport
		Deep Waters	
NADW	14°to 2°C	8 Sv	0.4 PW
AABW	2°to -1°C	10 Sv (30 Sv[a])	0.12 PW (0.36 PW[a])
Total	...	...	0.52 PW (0.76 PW)
		Intermediate Waters	
LSW	14°to 3°C	8 Sv	0.3 PW
NPIW	12°to 5°C	5 Sv	0.16 PW
AAIW (Atlantic-Indian)	14°to 4°C	10 Sv	0.4 PW
AAIW (Pacific)	14°to 4°C	4 Sv	0.2 PW
SEISAMW	14°to 9°C	5 Sv (10 Sv[b])	0.1 PW (0.2 PW[b])
Total	...	...	1.2 PW (1.3 PW)

[a] *Schmitz* [1995]
[b] Calculation here.

ature difference between incoming and outgoing flow. For instance, the commonly-calculated meridional heat transports across subtropical latitudes use mass balance through the entire vertical section. Meridional heat transports in the South Pacific and South Indian Oceans must contend with the net flow around Australia and therefore "complete" sections include the Indonesian throughflow region.

Heat transport can also be computed meaningfully for portions of the circulation which conserve mass. In the present treatment, the overturning circulation is separated into shallow, intermediate and deep components, each of which conserves mass with equal inflow (at some high temperature) and outflow (at a lower temperature). When, on the other hand, a quantity like heat transport is calculated for a portion of the circulation which on its own does not conserve mass, for instance the transport of the Gulf Stream or the Ekman layer transport, it is common to use degrees Celsius and refer to the quantity as "temperature transport" which is a misnomer since the units are Watts. However, the phrase does at least highlight the meaninglessness of the transport until it is taken together with another portion of the circulation which allows mass to be balanced.

Two approaches are taken here to computing heat transport associated with different parts of the overturn. First (section 3.1), heuristic estimates of the contributions of all intermediate and deep waters to overturn are calculated, based on formation rates and source and final temperatures for each water mass. Published direct heat transport estimates for sections at 30-32°S and 24°N are then used to calculate the overturning heat transport due to the shallow subductive subtropical gyre overturn. This calculation is done for the whole globe. Secondly (section 3.2) meridional heat transport is calculated directly for each of the overturning elements across 24°N using *Reid's* [1994, 1997] total velocity fields. This second approach is being extended now to the southern hemisphere where interpretation is more difficult because of ambiguities in defining shallow and intermediate water overturn and because of the connections between the three subtropical gyres through the Indonesian passages and south of Africa.

Neither of these two methods is concerned with the details of the transformation of waters from source to final properties: the heuristic method is much too simple, assuming a single temperature for the source and final properties, while the direct method looks only at northward and southward flow across a single latitude. The details do matter, however, when one considers the response of heat transport to changes in surface forcing.

3.1. Heuristic Structure of the Overturning Heat Transport

The relative sizes of heat transport associated with deep and intermediate water formation can be estimated from their source and final temperatures and formation rates. Each deep and fresh intermediate water mass is examined in the next few paragraphs.

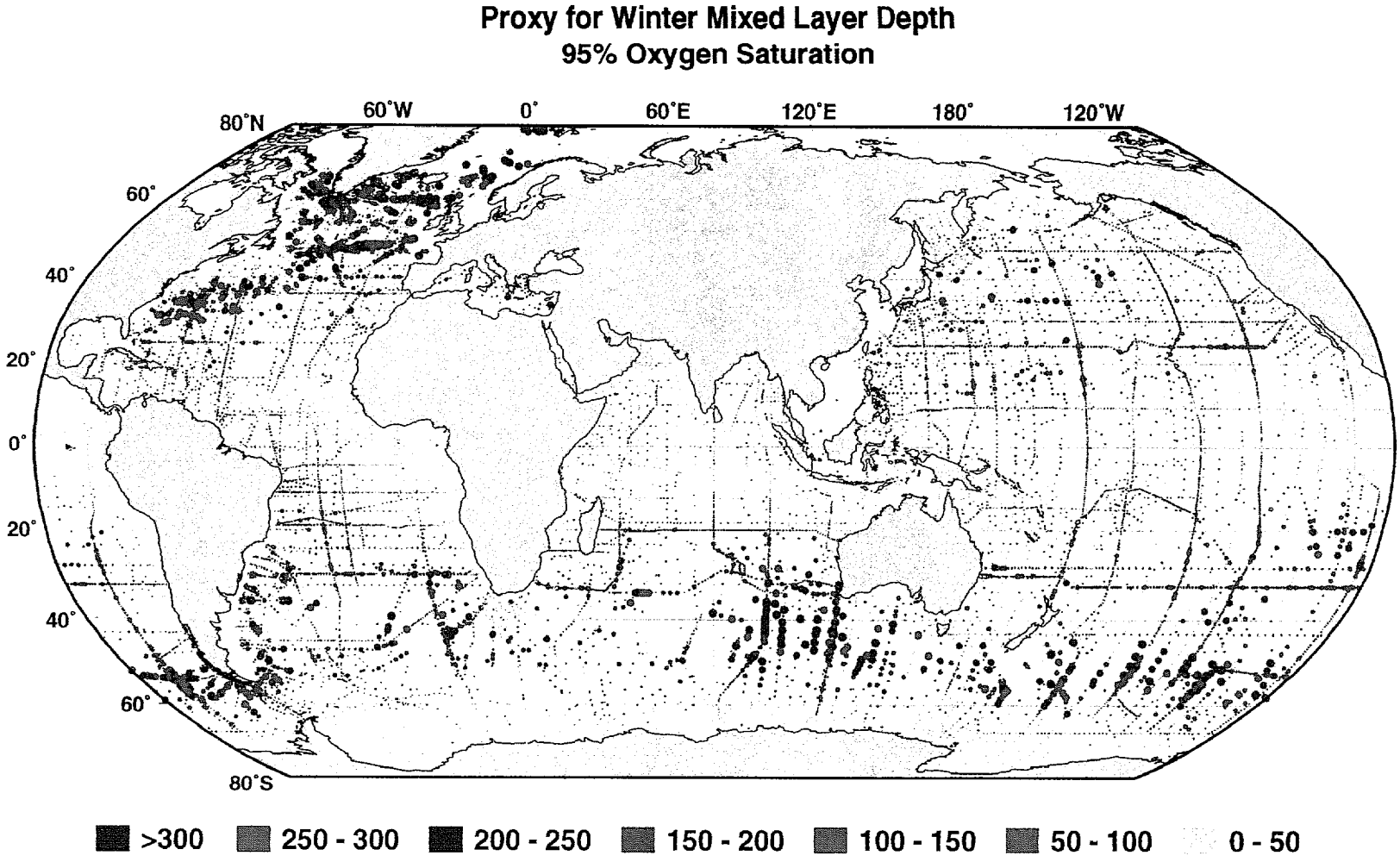

Plate 1. Depth of 95% oxygen saturation (m), based on historical hydrographic data and more recent WOCE hydrographic data. This depth is a crude proxy for the wintertime mixed layer depth, after *Reid's* [1982] more careful analysis for the North Pacific.

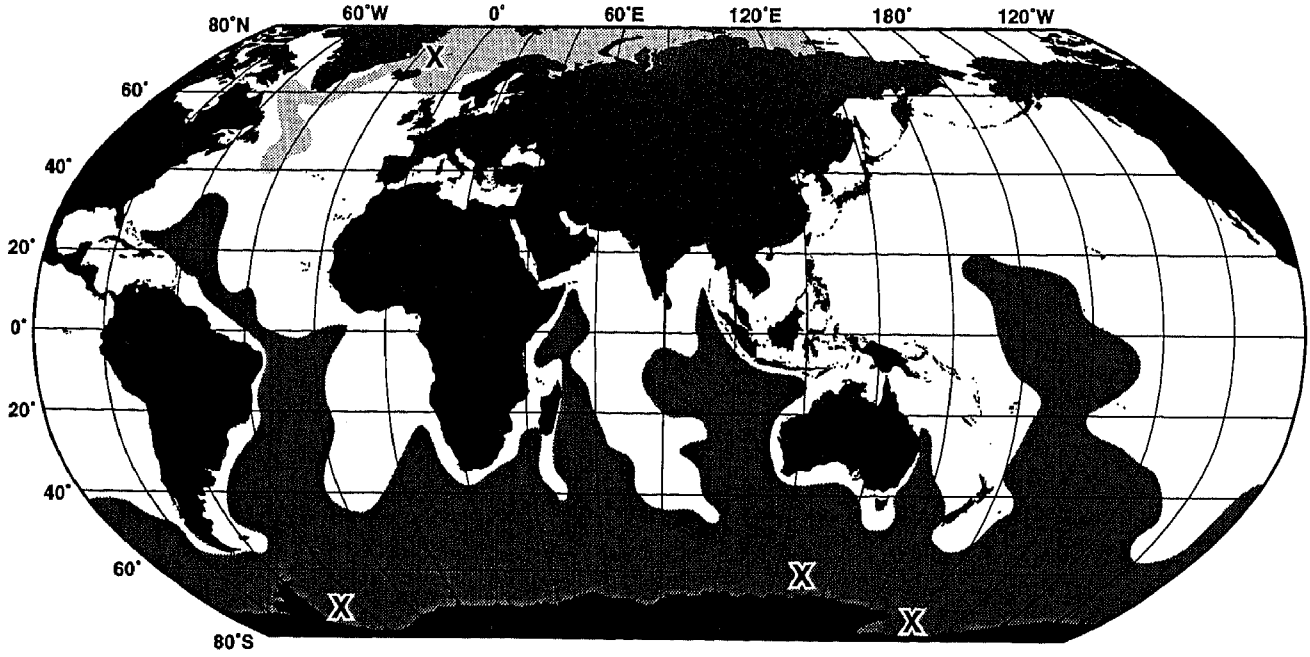

Figure 4. Location of the $\sigma_4 = 45.92$ kg m^{-3} isopycnal, representing the northward extent of the shallowest deep waters of Antarctic origin (dark shading) which can be unambiguously separated from those of North Atlantic origin (light shading). X's are formation regions for dense Antarctic waters. At lower densities, Antarctic water may be present but is not separated laterally from NADW in the North Atlantic.

As described in section 2, in the northern North Atlantic a thick layer of water of approximately 14°C is found east of the North Atlantic Current. *McCartney and Talley* [1982] define this as the warmest type of Subpolar Mode Water (SPMW), which is at the beginning of the process of cyclonic flow and gentle cooling around the subpolar gyre that eventually results in significant input into the Nordic Seas component of North Atlantic Deep Water (NADW) and production of Labrador Sea Water (LSW). The 14°C water cools as it is advected eastward; a portion splits northward into the subpolar gyre with the remainder staying in the subtropical gyre. For the heat budget, the details of this transformation are not important. A rough heat budget associated with NADW (Table 2) assumes an input temperature of 14°C, an outflow temperature of 2°C and a production rate of 8 Sv (1 Sv = $10^6 m^3/sec$) [*Worthington,* 1976; *McCartney and Talley,* 1984; *Dickson and Brown,* 1994; *Schmitz,* 1995]. Hence the estimated heat transport for this closed NADW mass balance is 0.4 PW. A rough heat budget for LSW assumes an input temperature of 14°C, an output temperature of 3°C, and a production rate of 8 Sv [*McCartney and Talley,* 1984; *Schmitz,* 1995], with an estimated heat transport of 0.3 PW. (Heat transports are quoted to tenths in the text although for calculations and in the tables they are carried in hundredths. An error estimate is difficult for such a rough calculation, but is expected to be on the order of 0.1 to 0.2 PW.)

If the 14°C SPMW, assumed as the main source of NADW and LSW, arises directly from water of about this temperature in the mid-subtropical gyre (hence in the Gulf Stream), with no input from warmer Gulf Stream waters, then the total heat transport of 1.2 PW which has been estimated directly across 24°N [*Hall and Bryden,* 1981; *Roemmich and Wunsch,* 1985; *Parilla et al.,* 1994] would be composed of about 0.7 PW due to NADW and LSW formation with the remaining 0.5 PW due to shallow overturn within the subtropical gyre. In section 3.2 below, the maximum heat transport associated with the shallow gyre overturn at 24°N is shown to be less than 0.3 PW, and thus the LSW/NADW heat transport is greater than 0.9 PW. Much of the water which feeds the NADW originates from Gulf Stream waters warmer than 14°C, with transformation to a lower temperature within the North Atlantic's subtropical (Gulf Stream and North Atlantic Current) circulation.

Table 3. Residual Shallow Gyre Overturn Heat Transports

Ocean	Direct Heat Transport Reference	Total Direct Heat Transport Estimate	Deep and Intermediate Water Heat Transports from Table 2	Residual Shallow Heat Transport
N. Atlantic	*Hall and Bryden* [1985]	1.2 PW	0.73 PW	0.47 PW
N. Atlantic	*Reid* [1994] and §3.2	1.18 PW		0.45 PW
N. Pacific	*Bryden et al.* [1991]	0.75 PW	0.16 PW	0.6 PW
N. Pacific	*Reid* [1998] and §3.2	0.63 PW		0.5 PW
S. Atlantic	*Rintoul* [1991]	0.25 PW	0.73-0.24 = 0.5 PW	-0.25 PW
S. Atlantic	*Rintoul* [1991]	0.25 PW	0.73-0.33 = 0.4 PW	-0.15 PW
S. Pacific	*Wunsch et al.* [1983]	-0.2 PW	0.2-0.24 = -0.04 PW	-0.16 PW
S. Pacific	*Wunsch et al.* [1983]	-0.2 PW	0.2-0.33 = -0.13 PW	-0.07 PW
Indian	*Robbins and Toole* [1995]	-0.4 PW	-0.35 PW	-0.05 PW
Indian	*Robbins and Toole* [1995]	-0.4 PW	-0.53 PW	0.13 PW

These heat transports (negative southward) are based on Table 2 and published direct heat transport estimates for 24°N and 30°S. South Atlantic and South Pacific deep/intermediate transports are the sum of their northern hemisphere deep/intermediate waters with an apportionment for southern hemisphere AABW and AAIW; upper and lower lines use minimum and maximum southern hemisphere transports from Table 2. The various use of one and two-place precision reflects the various estimates that go into the calculation, and should not be taken too literally.

The North Pacific forms intermediate water but not deep water. The warm water source for North Pacific Intermediate Water (NPIW) could be considered to be the thick layer of 10 - 12°C water found north of the Kuroshio. As in the North Atlantic, this thick layer advects eastward and a portion turns northward into the subpolar gyre, with maximum density occurring in the Okhotsk Sea due to brine rejection under sea ice formation and hence near the freezing point. The input to NPIW, however, is a mixture of the new dense water due to sea ice production and North Pacific waters produced through very strong tidal mixing at the Kuril Straits [*Talley,* 1991]. Thus 5°C, rather than a much colder temperature, is assigned here to the NPIW. Using an NPIW production rate of 5 Sv [*Talley,* 1997], the associated overturning heat transport is 0.2 PW (Table 2).

A heat transport of 0.75 PW across 24°N in the Pacific has been directly estimated by *Bryden et al.* [1991] and *Roemmich and McCallister* [1989] using a 1985 CTD section. (In section 3.2, the same data set with *Reid's* [1998] velocity analysis yields a direct heat transport estimate of 0.63 PW.) Thus the heat transport across this latitude due to shallow overturning might be 0.5-0.6 PW (Table 3). The complete calculation in section 3.2 below substantiates this heuristic argument, as does the analysis of *Bryden et al.* [1991].

In the southern hemisphere, Antarctic Intermediate Water is considered here to begin as a thick layer of Subantarctic Mode Water with an approximate temperature of 14°C east of the Brazil/Falkland Current confluence [*McCartney,* 1977]. Its final temperature just west of Chile is 4°C. Its formation rate is taken at 14 Sv [*Schmitz,* 1995], of which 4 Sv remains in the Pacific and 10 Sv passes through Drake Passage to enter the Atlantic/Indian gyre. The heat transport associated with AAIW formation is thus 0.6 PW (Table 2).

Southeast Indian Subantarctic Mode Water (SEISAMW) is similar dynamically to Pacific Antarctic Intermediate Water, and so a separate accounting for its heat transport is included here (see section 2.2 above). Its temperature is about 9°C and its formation rate is about 5 Sv according to *Schmitz* [1995]. The new WOCE sections which enclose the southeastern Indian Ocean can be used to compute SEISAMW export to the west and north in the Indian Ocean, with both a box at 32°S and 95°E and a closed section at 110°E. Both of these closed sections yield about 12 Sv of flow in the potential density range σ_θ = 26.7-26.9 into the Indian Ocean, with about half in the σ_θ = 26.7-26.8 and the other half in the σ_θ = 26.8-26.9 range. Therefore a larger transport of 10 Sv is used. If it is assumed that SEISAMW, like AAIW, originates at about 14°C, then the associated overturning heat transport is 0.1 PW or 0.2 PW for 5 Sv or 10 Sv, respectively (Table 2).

Antarctic Bottom Water (AABW) likely originates from NADW/Circumpolar Deep Water that upwells south of the Antarctic Circumpolar Current. The input

temperature is about 2°C. The outflow temperature is about -1°C. With a production rate of 10 Sv, the associated overturning heat transport is about 0.1 PW (Table 2). However, *Schmitz* [1995] shows a net production rate of about 30 Sv, when both the Weddell and Ross Sea sources are considered; a source along Adelie Land has also been substantiated [*Rintoul,* 1998]. With this large net export rate of 30 Sv of AABW, the net overturning heat transport associated with its production could be as much as 0.4 PW (Table 2).

Partitioning the overturning heat transports across the southern hemisphere basins at 30°S where direct estimates of heat transport have been made is difficult because the basins are connected. The first assumption is that the overturning heat transports calculated across the northern hemisphere lines for NPIW, NADW and LSW are assigned to the southern hemisphere sections, and hence that the 12°- 14°C water that is the northern hemisphere source originates at the same temperature in the southern hemisphere. Secondly, it is assumed here that the overturning heat transport associated with AAIW and AABW formation is divided equally between the three southern hemisphere oceans.

The direct heat transport estimate of 0.25 PW northward across 32°S in the South Atlantic [*Rintoul,* 1991] is thus divided here into 0.73 PW northward due to LSW and NADW formation, -0.2 PW (southward) due to AAIW and -0.1 PW due AABW formation. The remaining -0.2 PW of southward transport is then ascribed to shallow overturn in the subtropical gyre (Table 3).

The direct heat transport of -0.2 PW southward across 28°S in the South Pacific [*Wunsch et al.,* 1983] was based on a circulation with only a small Indonesian throughflow. The South Pacific heat transport is partitioned here into 0.2 PW northward due to NPIW formation, -0.2 PW (southward) due to AAIW formation in the Pacific and -0.1 PW due to AABW formation. These estimates leave -0.1 PW southward for the remaining shallow gyre overturn in the South Pacific, exclusive of the AAIW formation there. Note that *Wunsch et al.* [1983] indicated that their heat transport is indistinguishable from 0 PW, and so the non-AAIW shallow overturn could also be indistinguishable from 0.

In the Indian Ocean, the heat gain of -0.4 PW north of 32°S [*Robbins and Toole,* 1997] is balanced by export of heat across the two-part section composed of the 32°S section and one across the Indonesian throughflow. This net export of 0.4 PW is divided here into -0.2 PW southward due to AAIW formation, -0.1 PW due to AABW formation, and -0.1 to -0.2 PW southward due to SEISAMW formation (Table 3). This budget leaves 0.03 to -0.07 PW, indistinguishable from 0, for additional shallow gyre overturn, suggesting that SEISAMW formation dominates the shallow overturn.

Despite the limitations of these calculations, which are only partially supported by the direct heat transport estimates of section 3.2 below, one robust conclusion can be drawn: the global meridional heat transport associated with the formation of deep and bottom waters (NADW and AABW) is not significantly larger than the heat transport associated with formation of intermediate waters (LSW, NPIW, AAIW and SEISAMW). Even if only LSW and NPIW are considered as intermediate waters, the net heat transport associated with them is comparable to that for the deep waters. The input waters for each of these water masses, with the exception of AABW, are warm, on the order of 12 to 14°C, and the outflowing waters are on the order of 2 to 5°C. The temperature differences between inflow and outflow are of the same order. The total transformation rates are of the same order. Therefore the overturning heat transports associated with the deep and intermediate waters are about the same size.

The meridional heat transport associated with the shallow overturning gyres appears to be larger in the northern hemisphere oceans than in the southern hemisphere oceans, although as seen below, actually only the North Pacific's shallow overturn is significant. Weaker gyre strength and weaker surface buoyancy loss in the southern hemisphere subtropical gyres might be the cause of the difference. Or it could be that AAIW and SEISAMW dominate shallow overturn in southern hemisphere, although they were counted here as intermediate water formation.

3.2. Direct Estimates of Heat Transport in the Northern Hemisphere

Ocean heat transport has been estimated directly from ocean velocity (geostrophic and Ekman) and temperature information along zonal sections crossing each of the subtropical gyres. Absolute geostrophic velocities for the sections represented by arrows in Figure 1 have been estimated using inverse models with varying constraints [*MacDonald and Wunsch,* 1996 for all oceans; *Roemmich and McCallister,* 1989 for the North Pacific; *Roemmich and Wunsch,* 1985 for the North Atlantic; *Wunsch et al.,* 1983 for the South Pacific; *Rintoul,* 1991 for the South Atlantic; *Robbins and Toole,* 1997 for the Indian Ocean]. Geostrophic reference velocities were selected in a more traditional way based on water mass analysis and relative flow patterns for

several of the same sections [*Bryden et al.*, 1991 for the North Pacific; *Toole and Warren*, 1993 for the Indian; *Reid*, 1994 for the Atlantic sections; *Reid*, 1997 for the Pacific sections]. The method employed by *Hall and Bryden* [1982] for the North Atlantic zonal section took advantage of the zonal uniformity of vertically-averaged potential temperature along 24°N, allowing them to calculate the heat transport using only the baroclinic velocities rather than the absolute velocities.

The direct estimates presented here include only the two northern hemisphere subtropical gyres and are based on *Reid's* [1994, 1997] adjusted geostrophic velocities. CTD stations were occupied in 1981 along 24°N in the North Atlantic [*Roemmich and Wunsch*, 1985] and in 1985 along 24°N in the North Pacific [*Roemmich et al.*, 1991]. The North Atlantic section ends at the Bahamas in the west and is completed across the Gulf Stream at 26°N. The data (pressure, temperature, salinity) resolution is 2 dbar in the vertical. *Reid* [1994, 1997] included these two sections in his basin-wide flow analyses. He graciously provided files with his velocity solution at the deepest common level for each station pair. Reid assumed geostrophic mass balance across each section. For this study, Reid's velocities were adjusted to allow total mass balance to include Ekman transport, as described below.

The goal here is to estimate the contribution to the overturning heat transport due to shallow, intermediate and deep components. The shallow overturn is defined to extend down to the maximum density which is found at the sea surface in winter at the subtropical/subpolar gyre boundary, as defined by the Sverdrup transport. It is assumed that this is the maximum density of subducted overturn in the subtropical gyre (*Stommel's* [1979] Ekman demon concept). This assumption seems reasonable since even if there is baroclinic exchange across the gyre boundary, it most likely takes the form of southward Ekman transport of surface water (hence the densest surface water at the gyre boundary) and northward return flow of underlying water. Thus the shallow overturn is confined to the subducted portion of the subtropical gyre. This approach was taken by *Roemmich and Wunsch* [1985] for the North Atlantic 24°N section.

Once the maximum potential density for subduction is selected (σ_θ = 26.2 for the North Pacific and σ_θ = 27.3 for the North Atlantic), the mass transport across the subtropical zonal section is computed for this uppermost layer, including the geostrophic and Ekman components. The transport is divided between the northward western boundary current (Gulf Stream/Kuroshio) and the southward interior flow. Since the zero of northward Ekman transport lies at about 30°N and since all (northward) Ekman transport at 24°N is at much lower density than the maximum subducted density, it is assumed that all Ekman flow at 24°N loses buoyancy and joins the southward geostrophic flow of the subtropical gyre, with none continuing into the subpolar gyre. The mass balance required for a net heat transport for the shallow overturn is taken to be: (1) all northward Ekman transport at 24°N, (2) all southward geostrophic flow in the interior, and (3) the portion of the northward geostrophic flow in the western boundary current in this shallow layer that is required to balance mass, that is,

$$V_{wbcshall} = V_{ek} + V_{geointshall} \quad (1)$$

The remaining (geostrophic) transport in the warm water layer of the western boundary current enters the subpolar gyre and returns as intermediate or deep water. This result is similar to *Roemmich and Wunsch's* [1985] approach to what they labelled as "shallow wind-driven circulation" (which is described here as the thermohaline overturning associated with the subducting subtropical part of the wind-driven circulation).

For heat transport in the shallow overturning associated with (1), the annually-averaged temperature at 30 m from *Levitus et al.* [1994] is used with the Ekman transport, and the measured temperature averaged between adjacent CTD stations is used with the adjusted geostrophic velocities. The western boundary current portion of the heat transport is assumed to be of the least dense (warmest) water down to the depth required for mass balance. This choice maximizes the meridional heat transport assigned to the shallow overturn. A reasonable minimum value is obtained by using the average temperature of the whole shallow layer of the western boundary current, which reduces the northward temperature transport assumed for the western boundary current component of the shallow overturn, as was done by *Roemmich and Wunsch* [1985].

The intermediate and deep water overturning contributions to the heat transport across 24°N are described in the individual calculations below, where it is assumed that up and downwelling occur to the closest possible density for mass balance.

3.2.1. North Pacific. Hydrographic station data at 24°N in the Pacific were collected in 1985 [*Roemmich et al.*, 1991]. Meridional heat transport was calculated using an inverse method by *Roemmich and McCallister* [1989], who obtained 0.75 PW northward. The same heat transport was also calculated using adjusted refer-

ence velocities by *Bryden et al.* [1991]. (In comparison, *MacDonald and Wunsch* [1996] included the section in a global inverse model, and obtained 0.45 PW. Because regional attention was paid to initial reference velocity choices in the earlier papers which treated only the Pacific 24°N section, the earlier estimates were used in the heuristic treatment of section 3.1 above.)

Reid [1997] used the 24°N section in his Pacific circulation analysis and provided his set of bottom velocities (adjustments) for the present calculation. He assumed a net geostrophic mass balance across the section. Ekman transport across 24°N from *Hellerman and Rosenstein's* [1983] annually-averaged winds is 10.3 Sv northward. To adjust Reid's geostrophic transport to 10.3 Sv southward, a southward velocity correction of -0.0135 *cm/sec* was applied at all points of the section so that the geostrophic and Ekman transports sum to 0. (A similarly ad hoc adjustment was made by *Bryden et al.* [1991] for their estimate of heat transport at 24°N in the North Pacific.) The total, top-to-bottom, meridional heat transport across 24°N, using Reid's velocities adjusted as described and the Ekman transport, is (Table 4 and Figure 5)

$$\begin{aligned} H_{tot} = 0.63PW &= H_{ek} + H_{geostrophic} \\ &= 0.94PW - 0.31PW \end{aligned} \quad (2)$$

where the "heat" transports on the right hand side are relative to 0°C, and are referred to henceforth as "temperature transports", following *Hall and Bryden* [1982]. The heat transport on the left-hand side is associated with a complete mass balance and hence is a true net heat transport.

The maximum potential density of shallow overturn is $\sigma_\theta = 26.2$, based on the density at the zero of Sverdrup transport in the North Pacific [e.g., *Yuan and Talley,* 1992]. The shallow overturning heat transport, depicted in Figure 5b, is associated with the mass (volume) balance (Table 4):

$$\begin{aligned} V_{shallow} = 0Sv &= V_{wbcshall} + V_{ek} + V_{geointshall} \\ &= 21.5Sv + 10.3Sv - 31.8Sv \end{aligned} \quad (3)$$

$$\begin{aligned} H_{shallow} = 0.57PW &= H_{wbcshall} + H_{ek} + H_{geointshall} \\ &= 1.87PW + 0.94PW - 2.24PW. \end{aligned} \quad (4)$$

Again the heat transport on the left side is a true, net heat transport involving mass balance, while terms on the right side are temperature transports relative to 0°C. The Kuroshio (western boundary current) transport of 21.5 Sv required to balance the interior and Ekman transports is assumed to be of the least dense portion of the current, which is calculated from the data set to be all water of potential density less than $\sigma_\theta = 26.0$. This shallow heat balance leaves a small residual (lower bound) heat transport of 0.09 PW associated with intermediate water formation and deep overturn, which is now examined in detail.

The vertical mass overturn of the North Pacific was depicted by *Roemmich and McCallister* [1989] and *Bryden et al.* [1991] using zonally-integrated mass transports in pressure and potential temperature layers, respectively. The zonally integrated mass transport in potential density layers using *Reid's* [1997] velocities plus the correction made here for Ekman transport is shown in Figure 5c. The layers here were chosen to contain commonly-defined water masses. The layer boundaries are: the sea surface, $\sigma_\theta = 26.2$ for the maximum ventilated subtropical potential density as described above, $\sigma_\theta = 27.0$ lying between North Pacific Intermediate Water (NPIW) and Antarctic Intermediate Water (AAIW), $\sigma_\theta = 27.6$ between AAIW and Pacific Deep Water (PDW), $\sigma_2 = 36.96$ and $\sigma_4 = 45.84$ within the PDW, and $\sigma_4 = 45.88$ between the PDW and Lower Circumpolar Deep Water (LCDW, also known as Antarctic Bottom Water).

The main features of the mass transports here are similar to the previous depictions: northward Ekman transport, southward transport in the upper ocean, southward transport in the NPIW layer, northward transport in the AAIW layer, southward transport in the PDW, which is highest in the layer just above the LCDW, and northward transport of LCDW. The upper two PDW layers have very little transport, a feature also seen in the previous analyses.

The 3.1 Sv of northward-flowing bottom water must upwell and return southward across the section. This is assumed to be into the next layer up, of Pacific Deep Water, where the transport is -5.9 Sv. Assume that the temperature transport in this second layer is $\frac{3.1}{5.9}$ of the total temperature transport, given no information on exactly where the return of the deepest water occurs. Then the southward heat transport associated with this deep upwelling is

$$\begin{aligned} H_{bottom} = -0.002PW &= H_{LCDW} + \tfrac{3.1}{5.9} H_{PDW3} \\ &= 0.012PW - 0.014PW \end{aligned} \quad (5)$$

where LCDW refers to the bottom layer and PDW3 refers to the deepest of the three Pacific Deep Water layers.

Table 4a. Overall Volume, "Temperature" (T) and Heat Transports for 24°N

	North Pacific		North Atlantic	
	Volume (Sv)	Heat (PW)	Volume (Sv)	Heat (PW)
Ekman	10.3 Sv	0.94 PW (T)	5.5 Sv	0.43 PW (T)
Total Geostrophic	-10.3 Sv	-0.31 PW (T)	-5.5 Sv	0.75 PW (T)
Total	0.0 Sv	0.63 PW	0.0 Sv	1.18 PW

These estimates use *Reid's* [1994, 1998] velocity analyses, adjusted here to balance Ekman transport. (T) indicates temperature transport, as defined in the text.

Table 4b. Shallow and Intermediate/Deep Volume and Heat Transports for 24N

	North Pacific		North Atlantic	
	Volume (Sv)	Heat (PW)	Volume (Sv)	Heat (PW)
Ekman	10.3 Sv	0.94 PW (T)	5.5 Sv	0.43 PW (T)
Shallow Interior Geostrophic	-31.8 Sv	-2.24 PW (T)	-18.7 Sv	-1.54 PW (T)
Shallow Western Boundary Current Compensating Ekman and Shallow Interior	21.5 Sv	1.87 PW (T)	13.2 Sv	1.40 PW (T)
Shallow Layer Overturn Total	0.0 Sv	0.57 PW	0.0 Sv	0.29 PW
Intermediate/Deep Geostrophic	-1.6 Sv	-0.03 PW (T)	-15.8 Sv	-0.12 PW (T)
Shallow Western Boundary Current Compensating Intermediate and Deep Interior	1.6 Sv	0.09 PW (T)	15.8 Sv	1.01 PW (T)
Intermediate/Deep Overturn Total	0.0 Sv	0.06 PW	0.0 Sv	0.89 PW

These estimates use *Reid's* [1994, 1998] velocity analyses, adjusted here to balance Ekman transport. (T) indicates temperature transport, as defined in the text.

A downwelling of 2.8 Sv from the AAIW layer (σ_θ = 27.0-27.6) to the near-bottom layer is required to balance deep mass in this scheme. In *Roemmich and McCallister* [1989] there was almost complete mass balance in the bottommost two layers (northward at the bottom and compensating southward just above). Using Reid's analysis with the adjustment for Ekman transport, there is more southward flow just above the bottom layer than needed to compensate for the northward bottom layer. This excess flow requires downwelling from intermediate depths to the near-bottom layer to balance deep mass. A similar problem, requiring downwelling, was noted by *Bryden et al.* [1991] in their net transports for this same section for which they suggested mixing as a solution, but which they also noted was somewhat inconsistent with the mass balance. Without an obvious physical mechanism for so much downwelling, there is likely an error in the

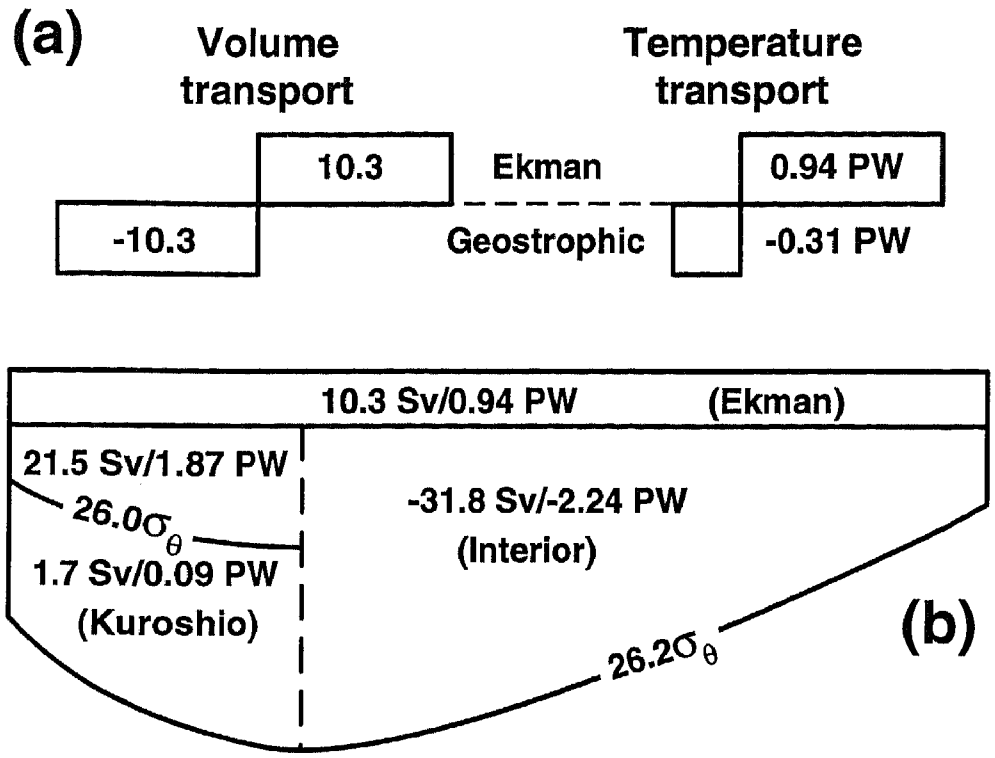
(a)
Volume transport
Temperature transport
10.3
Ekman
0.94 PW
-10.3
Geostrophic
-0.31 PW
10.3 Sv/0.94 PW (Ekman)
21.5 Sv/1.87 PW
26.0σθ
1.7 Sv/0.09 PW
(Kuroshio)
-31.8 Sv/-2.24 PW
(Interior)
26.2σθ
(b)

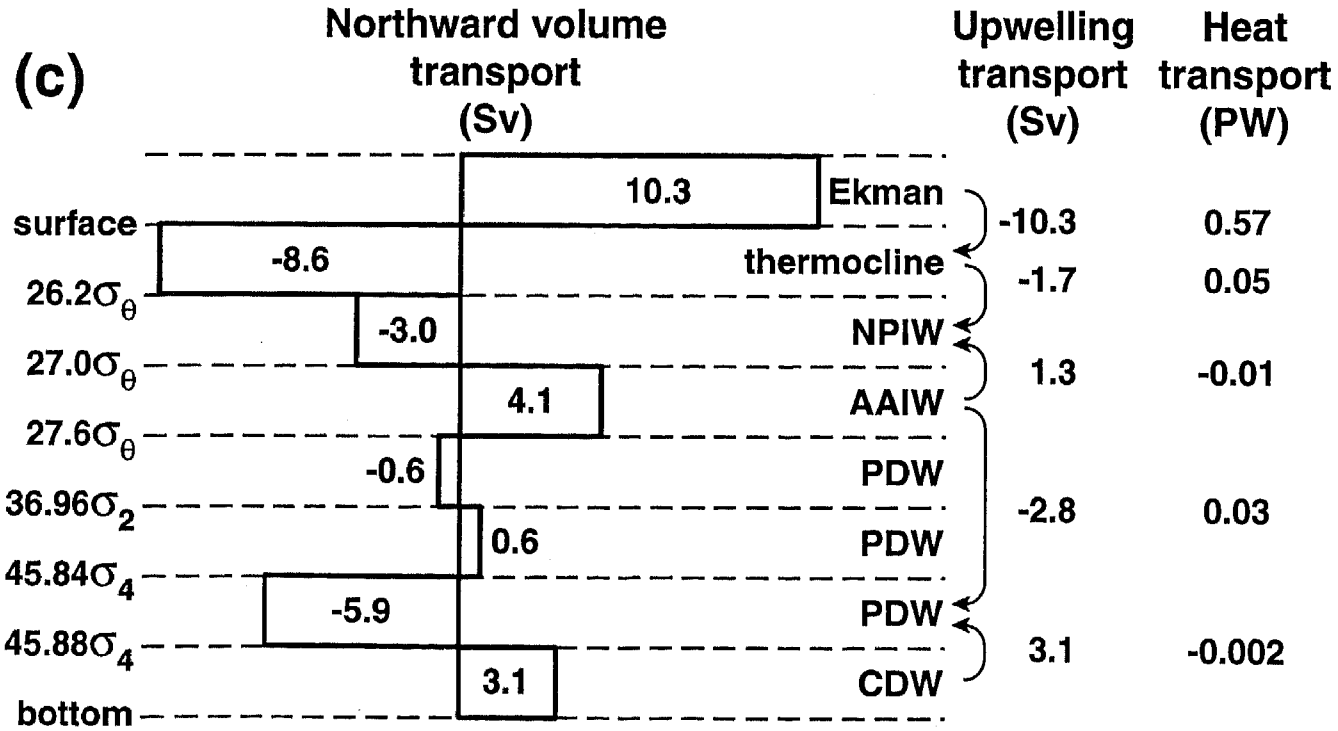
(c)
Northward volume transport (Sv)
Upwelling transport (Sv)
Heat transport (PW)
surface
26.2σθ
27.0σθ
27.6σθ
36.96σ2
45.84σ4
45.88σ4
bottom
10.3
Ekman
-8.6
thermocline
-3.0
NPIW
4.1
AAIW
-0.6
PDW
0.6
PDW
-5.9
PDW
3.1
CDW
-10.3
0.57
-1.7
0.05
1.3
-0.01
-2.8
0.03
3.1
-0.002

Figure 5. Direct heat transport estimate at 24°N in the Pacific, using *Reid's* [1997] absolute velocities, adjusted to zero mass balance using Ekman transport based on *Hellerman and Rosenstein's* [1983] annually-averaged winds. (a) Volume and temperature transports in the Ekman layer and total geostrophic flow. (b) Shallow overturning schematic, divided into the western boundary current, Ekman layer and southward interior geostrophic flow. The base of the shallow layer is at $\sigma_\theta = 26.2$ kg m^{-3}. The Kuroshio transport is divided in two: 21.5 Sv required to balance the Ekman and interior return flow in this layer, and a 1.7 Sv residual which flows on into the subpolar gyre. "Temperature" transports (heat transports without mass balance) are relative to 0°C. The net heat transport for this mass-balanced shallow overturn is 0.47 PW. (c) Zonally-integrated transports in isopycnal layers (bar graph). Vertical arrows and transports indicate assumed transfer of mass between layers, assuming that mass moves preferentially to the most adjacent layer. The heat transports at the right are based on the mass balances implied by the upwelling transports, and so are the net heat transports associated with each part of the overturn.

mass transports. (In Reid's original velocities, unadjusted for Ekman mass balance, there is near balance between these two deepest layers, suggesting that the excess flow and hence downwelling is an artifact of the *ad hoc* correction applied here.) Since deep temperature differences are small, such an error in deep transport has little effect on heat transport, as noted by *Bryden et al.* [1991]. For the downwelling transport, assume again that the temperature transport contribution from the AAIW layer is simply proportional to its total temperature transport. This downwelling carries

$$\begin{aligned}\tfrac{2.8}{4.1}H_{AAIW} + \tfrac{3.1}{5.9}H_{PDW3} &= 0.04PW - 0.01PW \\ &= 0.03PW. \end{aligned} \quad (6)$$

Because the temperature difference between these two layers is small despite their large vertical separation, this heat transport, even if incorrect, is small compared with the total northward heat transport of 0.63 PW for the section.

The remaining 1.3 Sv of the northward AAIW transport must upwell into the NPIW layer, partially compensating the 3.0 Sv of southward NPIW transport. This upwelling has associated southward heat transport of

$$\begin{aligned}\tfrac{1.3}{3.0}H_{NPIW} + \tfrac{1.3}{4.1}H_{AAIW} &= -0.03PW + 0.02PW \\ &= -0.01PW. \end{aligned} \quad (7)$$

The remaining 1.7 Sv of southward flow in the NPIW layer is assumed to come from the surface layer of the western boundary current, so the associated heat transport is the difference between the total heat transport of 0.63 PW and all of these layer transports, or 0.05 PW.

Thus the partition of northward heat transport across 24°N in the Pacific into the shallow overturn, NPIW overturn, and deep water upwelling is 0.57 PW, 0.09 PW and -0.002 PW, respectively, plus the putative 0.03 PW of downwelling heat transport from AAIW to PDW.

This partitioning between shallow subtropical gyre overturn and intermediate water overturn resembles the heuristic calculation of section 3.1 above (Table 2), which was based on rough assumptions about the intermediate water formation rate and associated temperature change from inflow to outflow.

3.2.2. North Atlantic. Hydrographic data have been collected along 24°N in the Atlantic four times - 1957, 1981, 1992 and 1998. *Hall and Bryden* [1981] calculated a net heat transport of 1.22 PW across the 1957 section based on temperature transports of 0.42 PW due to northward Ekman transport, 2.38 PW due to the northward current in Florida Straits, and -1.58 PW due to the southward interior flow.

Roemmich and Wunsch [1985] used an inverse method to calculate a meridional heat transport of 1.2 PW across the 1957 and 1981 sections. They divided this into 0.1 PW for the shallow "wind-driven" circulation using 27.4 σ_θ as the bottom of the subducted flow, and 1.1 PW for the "thermohaline" circulation. In their global inverse, *Macdonald and Wunsch* [1996] calculated a northward heat transport of 1.1 PW for the 1981 24°N section. *Parrilla et al.* [1994] found a net heat transport of 1.2 PW for the 1992 section, very similar in size to the calculations for the 1981 section, despite a temperature increase of 0.1 to 0.2°C from 1981 to 1992 at Labrador Sea Water depths. Heat transports are sensitive only to much grosser temperature changes, as well as changes in the mass transport distribution, which apparently differed little between 1981 and 1992.

Reid [1994] used the 1981 24°N section in his circulation analysis of the Atlantic, and supplied the geostrophic velocities for this calculation. The section is composed of two portions: a Gulf Stream crossing at 26°N and the main section at 24°N between the Bahamas and the eastern boundary. As done for the North Pacific in section 3.1 above, an Ekman transport of 5.5 Sv was

calculated from the annually-averaged winds of *Hellerman and Rosenstein* [1983]. Since Reid's geostrophic mass was balanced, velocities here were adjusted at all points by -0.0118 cm/sec to balance the Ekman and geostrophic mass transports.

The total heat transport from Reid's geostrophic velocities with this correction applied, again using the 30 m annually-averaged temperature from *Levitus et al.* [1994] for the Ekman heat transport, is (Table 4a and Figure 6)

$$H_{tot} = 1.18PW = H_{ek} + H_{geostrophic} = 0.43PW + 0.75PW \quad (8)$$

which is the same total as from *Hall and Bryden* [1981], *Roemmich and Wunsch* [1985] and *Parilla et al.* [1994]. Here the net geostrophic mass transport is southward (-5.5 Sv), but the associated temperature transport (relative to a temperature of 0°C) is northward, unlike for the North Pacific.

Shallow overturn in the North Atlantic is defined to be confined to densities lower than $\sigma_\theta = 27.3$, based on the maximum surface density in the subtropical gyre [e.g. *McCartney*, 1982]. In this upper ocean layer, the southward geostrophic transport east of the Bahamas is -18.7 Sv. With a northward Ekman transport across 24°N of 5.5 Sv, 13.2 Sv of the total of 29.0 Sv of the Florida Strait Gulf Stream's upper layer transport is required to balance mass. 15.8 Sv of the Gulf Stream's upper layer continue northward to become part of the intermediate/deep overturn. It is next assumed that the Gulf Stream transport of 13.2 Sv that remains in the subtropical gyre is the warmest, least dense part of the Gulf Stream or all water less dense than $\sigma_\theta = 25.8$, with an associated temperature transport of 1.41 PW northward. The volume and heat balances for the subtropical subductive overturn, assuming that the Ekman transport and warmest Gulf Stream waters feed the southward interior flow, is then (Table 4b)

$$V_{shallow} = 0Sv = V_{wbcshall} + V_{ek} + V_{geointshall} = 13.2Sv + 5.5Sv - 18.7Sv \quad (9)$$

$$H_{shallow} = 0.30PW = H_{wbc} + H_{ek} + H_{interior} = 1.41PW + 0.43PW - 1.54PW. \quad (10)$$

as depicted in Figure 6b. This heat transport is somewhat less than the heuristic estimate (section 3.1) of 0.5 PW for the North Atlantic, and is likely an upper bound on the shallow heat transport, since it is assumed that the warmest Gulf Stream water stays in the subtropical gyre while the colder water in this shallow layer passes to the subpolar gyre. It is equally possible that some of the colder shallow water remains in the gyre; if it is assumed that the temperature transport for this surface to the $\sigma_\theta = 27.3$ layer is just a simple proportion of the total temperature transport in the Gulf Stream [as in *Roemmich and Wunsch*, 1983], the total heat transport for the shallow gyre overturn is reduced to about 0.0 PW. Similarly low heat transport for the shallow gyre was calculated by *Hall and Bryden* [1981] and *Roemmich and Wunsch* [1983].

The water column is next divided according to water masses to estimate the relative contribution of the remaining parts of the overturn to the total heat transport. The vertical distribution of zonally-integrated transport (Figure 6c) based on *Reid's* [1994] velocities is in keeping with that of *Roemmich and Wunsch* [1983], with a northward flux of 6.9 Sv of Antarctic Bottom Water (AABW), a southward flux of about 19 Sv of North Atlantic Deep Water (NADW), a southward flux of about 7 Sv of Labrador Sea Water (yielding a total southward flux of NADW plus LSW of about 26 Sv), and a net northward transport at the Antarctic Intermediate Water level and in the upper ocean.

Starting from the deepest layer, all 6.9 Sv of AABW must upwell, assumed to be into the southward-flowing NADW lying just above. The (southward) heat transport associated with this abyssal upwelling is -0.02 PW, which is small because of the small temperature difference between AABW and NADW.

The remaining 11.9 Sv of southward-flowing NADW and 6.5 Sv of LSW must be fed by downwelling from the surface and AAIW layers (water mass formation). The overturning heat transport associated with LSW is 0.43 PW and with NADW is 0.48 PW.

Thus the North Atlantic's meridional heat transport of 1.18 PW at 24°N is dominated by conversion of upper layer water into LSW and NADW, which contribute together 0.91 PW. In contrast, the North Pacific is dominated by the shallow overturning, as already concluded by *Hall and Bryden* [1981], *Roemmich and Wunsch* [1985] and *Bryden et al.* [1991]. The LSW overturning heat transport is a substantial fraction of the whole. However, the upper bound on the strength of the subtropical shallow overturn as calculated here is greater than in Roemmich and Wunsch and in Hall and Bryden, due to the assumption here that the Gulf Stream transport which feeds the shallow overturn is of the warmest waters. The upper bound on shallow overturning heat transport of 0.30 PW is lower than the

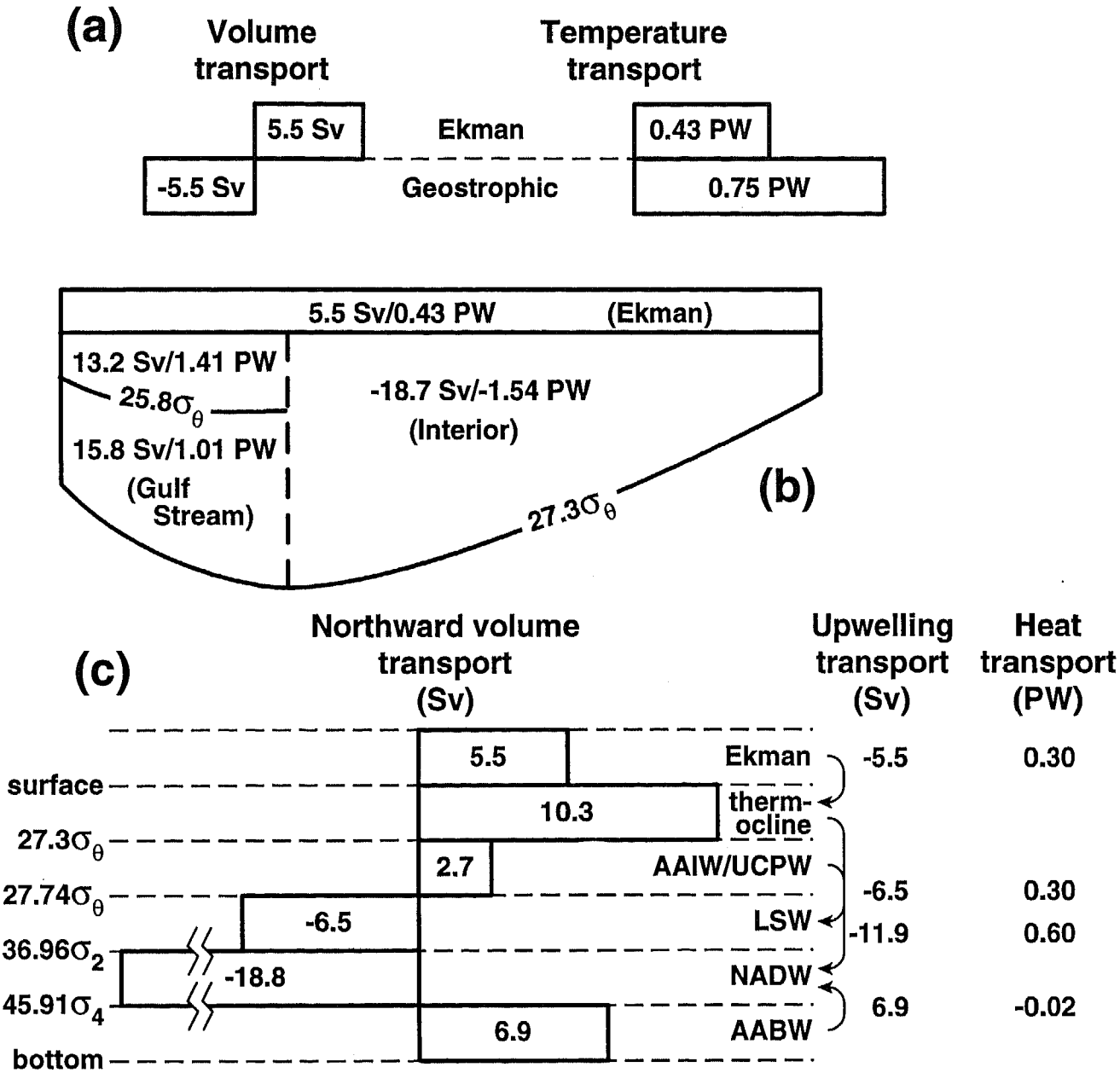

Figure 6. Direct heat transport estimate at 24°N in the Atlantic, using *Reid's* [1997] absolute velocities, adjusted to zero mass balance using Ekman transport based on *Hellerman and Rosenstein's* [1983] annually-averaged winds. (a) Volume and temperature transports in the Ekman layer and total geostrophic flow. (b) Shallow overturning schematic, divided into the western boundary current, Ekman layer and southward interior geostrophic flow. The base of the shallow layer is at $\sigma_\theta = 27.3$ kg m^{-3}. The Gulf Stream upper layer transport is divided in two, as in *Roemmich and Wunsch* [1985]: 22.1 Sv required to balance the Ekman and interior return flow in this layer, and 15.9 Sv residual which flows on into the subpolar gyre. "Temperature" transports (heat transports without mass balance) are relative to 0°C. The net heat transport for this mass-balanced upper layer overturn is 0.03 PW. (c) Zonally-integrated transports in isopycnal layers (bar graph). Vertical arrows and transports indicate assumed transfer of mass between layers, assuming that mass moves preferentially to the most adjacent layer. The heat transports at the right are based on the mass balances implied by the upwelling transports, and so are the net heat transports associated with each part of the overturn.

heuristic estimate of 0.47 PW for the shallow overturn (section 3.1), implying that the average temperature of surface/thermocline water that is transformed into LSW and NADW is greater than 14°C at 24°N.

4. DISCUSSION

Both the heuristic and more precise computations of the relative contribution of intermediate and deep waters to the global overturning heat transport reveal that intermediate water formation is responsible for about the same amount of heat transport as deep water formation. In the North Atlantic, intermediate and deep water formation are associated with at least 75% of the meridional heat transport across the subtropical gyre. The large heat loss near the Gulf Stream that is associated with Subtropical Mode Water formation functions as a step towards the complete and much denser total water mass formation of the northern North Atlantic and Nordic Seas. The North Pacific situation is exactly the opposite, with only weak intermediate water formation and no deep water formation. North Pacific shallow gyre overturn is responsible for about 75% of the meridional heat transport across the subtropical gyre.

In the southern hemisphere, Antarctic Intermediate Water (AAIW) formation involves a temperature change which is about three times larger than that for Antarctic Bottom Water (AABW) formation. If the formation rates of AAIW and AABW are roughly the same, AAIW formation would contribute more than AABW to global overturning heat transport.

AAIW formation in the southeastern Pacific is actually more akin to shallow subtropical gyre overturn than it is to the intermediate water formation of the northern hemisphere - it lies in the poleward-eastern side of the gyre and much of it is subducted equatorward around the subtropical gyre. Therefore, the shallow gyre overturn of the South Pacific is likely dominated by this water mass formation, with formation of less dense waters in the subtropical gyre mainly as precursors. The Subantarctic Mode Water of the southeastern Indian Ocean (SEISAMW) is dynamically and volumetrically similar to the southeast Pacific AAIW, and carries most of the shallow overturning heat transport of the Indian's subtropical gyre. The total contribution of SEISAMW to the global overturning transport is rather small since its temperature change from input to output water is about half that of the AAIW.

The good agreement between the heuristic and the direct estimates of shallow, intermediate and deep overturn in the northern hemisphere suggests that the crude assumptions made about the principal water masses, their temperatures and formation rates are reasonable and that these water masses actually do dominate the overturning heat transport. It is concluded that shallow, intermediate and deep overturning all contribute relatively equally to the global meridional heat transports. At a minimum, any simplified model or concept of the present or past states of the overturning circulation must include intermediate water formation. Even if Labrador Sea Water is considered to be part of North Atlantic Deep Water, Antarctic Intermediate Water and Antarctic Bottom Water cannot be so combined. In fact, because it is associated with a larger temperature change from source to outflow, Antarctic Intermediate Water formation likely contributes more to overturning heat transport than does Antarctic Bottom Water and cannot be ignored in a global analysis.

Acknowledgments

This study was supported by the National Science Foundation through grants OCE-9712209 and OCE-9529584. The absolute velocities used for the direct heat transport calculations were graciously supplied by J.L. Reid.

REFERENCES

Barnier, B., L. Siefridt and P. Marchesiello, Thermal forcing for a global ocean circulation model using a three-year climatology of ECMWF analyses, *J. Mar. Systems, 6,* 363-380, 1995.

Broecker W., The great ocean conveyor, *Oceanography, 4,* 79-89, 1991.

Bryden, H. L., D. H. Roemmich and J. A. Church, Ocean heat transport across 24-degrees-N in the Pacific, *Deep-Sea Res., 38,* 297-324, 1991.

Clarke, A., and J.-C. Gascard, The formation of Labrador Sea Water, Part I - Large scale processes, *J. Phys. Oceanogr., 13,* 1764-1778, 1983.

da Silva, A. M., C. C. Young and S. Levitus, Atlas of Surface Marine Data 1994. Vol. 3: Anomalies of Heat and Momentum Fluxes, NOAA Atlas NESDIS 8, U. S. Department of Commerce, NOAA, NESDIS, 413 pp., 1994.

Dickson, R. R. and J. Brown, The production of North Atlantic Deep Water: sources, rates and pathways, *J. Geophys. Res., 99,* 12319-12341, 1994.

Freeland, H. J., A. S. Bychkov, F. Whitney, C. Taylor, C. S. Wong and G. I. Yurasov, WOCE section P1W in the Sea of Okhotsk - 1. Oceanographic data description, *J. Geophys. Res., 103,* 15613-15623, 1998.

Gordon, A. L., Interocean exchange of thermocline water, *J. Geophys. Res., 91,* 5037-5046, 1986.

Gordon, A. L., J. R. E. Lutjeharms and M. J. Grundlingh, Stratification and circulation at the Agulhas Retroflection, *Deep-Sea Res., 34,* 565-600, 1987.

Hall, M. M. and H. L. Bryden, Direct estimates and mechanisms of ocean heat transport, *Deep-Sea Res., 29,* 339-359, 1982.

Hautala, S. L. and D. H. Roemmich, Subtropical mode water in the northeast Pacific basin, *J. Geophys. Res., 103,* 13055-13067, 1998.

Hsiung, J., Estimates of global oceanic meridional heat transport, *J. Phys. Oceanogr., 15,* 1405-1413, 1985.

Josey, S. A., E. C. Kent, D. Oakley and P. K. Taylor, A new global air-sea and momentum flux climatology, *Int'l. WOCE Newsletter, 24,* 3-5, 1996.

Käse, R., W. Zenk, T. B. Sanford, and W. Hiller, Currents, fronts and eddy fluxes in the Canary Basin, *Prog. Oceanogr., 14,* 231-257, 1985.

Keith, D. W., Meridional energy transport: uncertainty in zonal means, *Tellus, 47A,* 30-44, 1995.

Kitani, K., An oceanographic study of the Okhotsk Sea - particularly in regard to cold waters, *Bull. Far Seas Fish. Res. Lab., 9,* 45-76, 1973.

Lazier, J., Oceanographic conditions at Ocean Weather Ship Bravo, 1964-1974, *Atmos. Ocean., 18,* 227-238, 1980.

Levitus, S., and T. Boyer, World Ocean Atlas 1994, Vol. 4: Temperature, *NOAA Atlas NESDIS 4,* U.S. Department of Commerce, NOAA, NESDIS, Washington, D.C., 1994.

Luyten, J. R., J. Pedlosky, and H. Stommel, The ventilated thermocline, *J. Phys. Oceanogr., 13,* 292-309, 1983.

MacDonald, A. M., Property fluxes at 30°S and their implications for the Pacific-Indian throughflow and the global heat budget, *J. Geophys. Res., 98,* 6851-6868, 1993.

MacDonald, A. M. and C. Wunsch, An estimate of global ocean circulation and heat fluxes, *Nature, 382,* 436-439, 1996.

Mantyla, A. W., On the potential temperature in the abyssal Pacific Ocean, *J. Mar. Res., 33,* 341-354, 1975.

Mantyla, A. W., and J. L. Reid, Abyssal characteristics of the world ocean waters, *Deep-Sea Res., Part A, 30,* 805-833, 1983.

McCartney, M. S., Subantarctic Mode Water, in *A Voyage of Discovery, George Deacon 70th Anniversary Volume,* edited by M. Angel, pp. 103-119, Pergamon, Elmsford, N.Y., 1977.

McCartney, M. S., The subtropical recirculation of Mode Waters, *J. Mar. Res., 40,* suppl., 427-464, 1982.

McCartney, M. S. and L. D. Talley, The Subpolar Mode Water of the North Atlantic Ocean, *J. Phys. Oceanogr., 12,* 1169-1188, 1982.

McCartney, M. S. and L. D. Talley, Warm water to cold water conversion in the northern North Atlantic Ocean, *J. Phys. Oceanogr., 14,* 922-935, 1984.

Oort, A. H. and T. H. Vonder Haar, On the observed annual cycle in the ocean-atmosphere heat balance over the Northern Hemisphere, *J. Phys. Oceanogr., 6,* 781-800, 1976.

Parrilla, G. A., A. Lavín, H. Bryden, M. García and R. Millard, Rising temperatures in the subtropical North Atlantic Ocean over the past 35 years, *Nature, 369,* 48-51, 1994.

Reid, J. L., On the use of dissolved oxygen concentration as an indicator of winter convection, *Naval Research Reviews, 34,* 28-39, 1982.

Reid, J. L., On the total geostrophic circulation of the South Pacific Ocean: Flow patterns, tracers and transports, *Prog. Oceanogr., 16,* 1-61, 1986.

Reid, J. L., On the total geostrophic circulation of the North Atlantic Ocean: flow patterns, tracers and transports, *Progr. Oceanogr., 33,* 1-92, 1994.

Reid, J. L., On the total geostrophic circulation of the Pacific Ocean: Flow patterns, tracers and transports, *Prog. Oceanogr., 39* 263-352, 1997.

Reid, J.L. and R. J. Lynn, On the influence of the Norwegian-Greenland and Weddell seas upon the bottom waters of the Indian and Pacific oceans, *Deep-Sea Res., 18,* 1063-1088, 1971.

Rintoul, S. R., South Atlantic interbasin exchange, *J. Geophys. Res., 96,* 2675-2692, 1991.

Rintoul, S. R., On the origin and influence of Adelie Land bottom water, *Ocean, Ice and Atm. Interactions at the Antarctic Continental Margin, Ant. Res. Ser., 75,* 151-171, 1998.

Robbins, P. E. and J. M. Toole, The dissolved silica budget as a constraint on the meridional overturning circulation of the Indian Ocean, *Deep-Sea Res., 44,* 879-906, 1997.

Roemmich, D., Estimation of meridional heat flux in the North Atlantic by inverse methods, *J. Phys. Oceanogr., 10,* 1972-1983, 1980.

Roemmich, D., T. McCallister and J. Swift, A transpacific hydrographic section along latitude 24°N; the distribution of properties in the subtropical gyre, *Deep-Sea Res., 38 (Suppl.),* S1-S20, 1991.

Roemmich, D., and B. Cornuelle, The subtropical mode waters of the South Pacific Ocean, *J. Phys. Oceanogr., 22,* 1178-1187, 1992.

Roemmich, D. and T. McCallister, Large scale circulation of the North Pacific Ocean, *Prog. Oceanogr., 22,* 171-204, 1989.

Roemmich, D. and C. Wunsch, Two transatlantic sections: meridional circulation and heat flux in the subtropical North Atlantic Ocean, *Deep-Sea Res., 32,* 619-664, 1985.

Schmitz, W. J., On the interbasin-scale thermohaline circulation, *Rev. Geophys., 33,* 151-173, 1995.

Speer, K., Water mass formation from revised COADS data, *J. Phys. Oceanogr., 25,* 2445-2457, 1992.

Speer, K., and E. Tziperman, Rates of water mass formation in the North Atlantic Ocean, *J. Phys. Oceanogr., 22,* 93-104, 1992.

Stommel, H., Determination of water mass properties of water pumped down from the Ekman layer to the geostrophic flow below, *Proc. Nat. Acad. Sci., 76,* 3051-3055, 1979.

Suga, T., Y. Takei, and K. Hanawa, Thermostad distribution in the North Pacific subtropical gyre: The central mode water and the subtropical mode water, *J. Phys. Oceanogr., 27,* 140-152, 1997.

Swift, J. H., K. Aagaard, and S.-A. Malmberg, The contribution of the Denmark Strait overflow to the deep North Atlantic, *Deep-Sea Res., 27,* 29-42, 1980.

Talley, L. D., Meridional heat transport in the Pacific Ocean, *J. Phys. Oceanogr., 14,* 231-241, 1984.

Talley, L. D., Ventilation of the subtropical North Pacific: the shallow salinity minimum, *J. Phys. Oceanogr., 15,* 633-649, 1985.

Talley, L. D., An Okhotsk Sea water anomaly: implications for sub-thermocline ventilation in the North Pacific, *Deep-Sea Res., 38,* S171-190, 1991.

Talley, L. D., Distribution and formation of North Pacific Intermediate Water, *J. Phys. Oceanogr., 23,* 517-537, 1993.

Talley, L. D., Antarctic Intermediate Water in the South Atlantic, *The South Atlantic: Present and Past Circulation,* edited by G. Wefer, W.H. Berger, G. Siedler and D. Webb, Springer-Verlag, New York, 219-238, 1996a.

Talley, L. D., North Atlantic circulation, reviewed for the CNLS conference, *Physica D, 98,* 625-646, 1996b.

Talley, L. D., North Pacific intermediate water transports in the mixed water region, *J. Phys. Oceanogr., 27,* 1795-1803, 1997.

Talley, L. D., and M. S. McCartney, Distribution and circulation of Labrador Sea Water, *J. Phys. Oceanogr., 12,* 1189-1205, 1982.

Talley, L. D., Y. Nagata, M. Fujimura, T. Iwao, K. Tokihiro, D. Inagake, M. Hirai and K. Okuda, North Pacific Intermediate Water in the Kuroshio/Oyashio mixed water region in Spring, 1989, *J. Phys. Oceanogr., 25,* 475-501, 1995.

Toole, J. M. and B. A. Warren, A hydrographic section across the subtropical South Indian Ocean, *Deep-Sea Res., 40,* 1973-2019, 1993.

Tsuchiya, M., Circulation of Antarctic Intermediate Water in the North Atlantic Ocean, *J. Mar. Res., 47,* 747-755, 1989.

Tsuchiya, M., L. D. Talley and M. S. McCartney, Water mass distributions in the western Atlantic: a section from South Georgia Island (54S) northward across the equator, *J. Mar. Res., 52,* 55-81, 1994.

Wacongne, S., and R. Pacanowski, Seasonal heat transport in a primitive equation model of the tropical Indian Ocean, *J. Phys. Oceanogr., 26,* 2666-2699, 1996.

Wakatsuchi, M., and S. Martin, Satellite observations of the ice cover of the Kuril basin region of the Okhotsk Sea and its relation to the regional oceanography, *J. Geophys. Res., 95,* 13393-13410, 1990.

Worthington, L. V., On the North Atlantic circulation, *Johns Hopkins Oceanogr. Studies, 6,* 110 pp., 1976.

Wunsch, C., D. Hu and B. Grant, Mass, heat and nutrient fluxes in the South Pacific Ocean, *J. Phys. Oceanogr., 13,* 725-753, 1983.

Wüst, G., The stratosphere of the Atlantic Ocean, *Wiss. Erg. der Deutsch. Atl. Exp. auf dem Vermessungs- und Forschungsschiff Meteor 1925-1927, 6,* 109-288, 1935.

Yuan, X., and L. D. Talley, Shallow salinity minima in the North Pacific, *J. Phys. Oceanogr., 22,* 1302-1316, 1992.

L. D. Talley, Scripps Institution of Oceanography, 9500 Gilman Dr., 0230, La Jolla, CA 92093. (e-mail: ltalley@ucsd.edu)

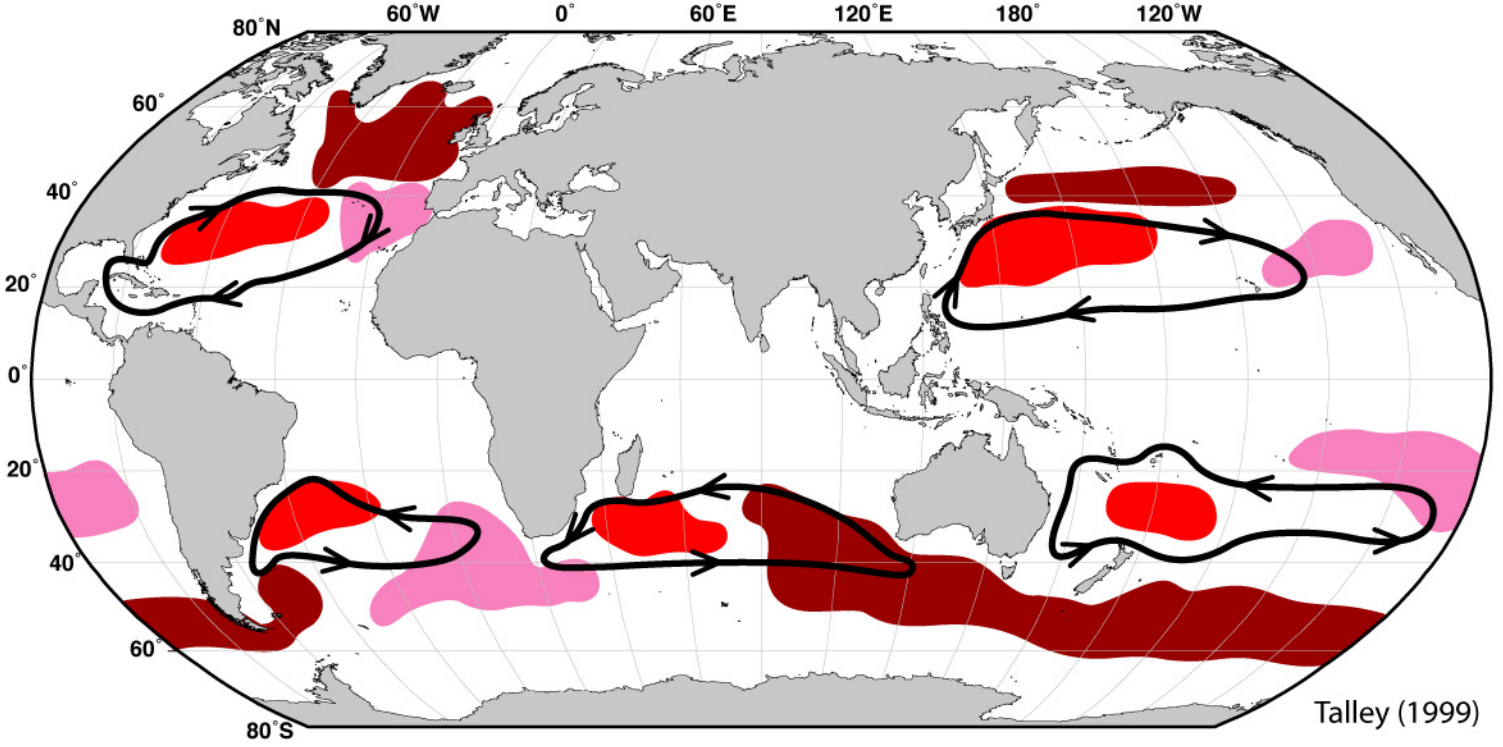
80°N
60°W
0°
60°E
120°E
180°
120°W
60°
40°
20°
0°
20°
40°
60°
80°S
Talley (1999)

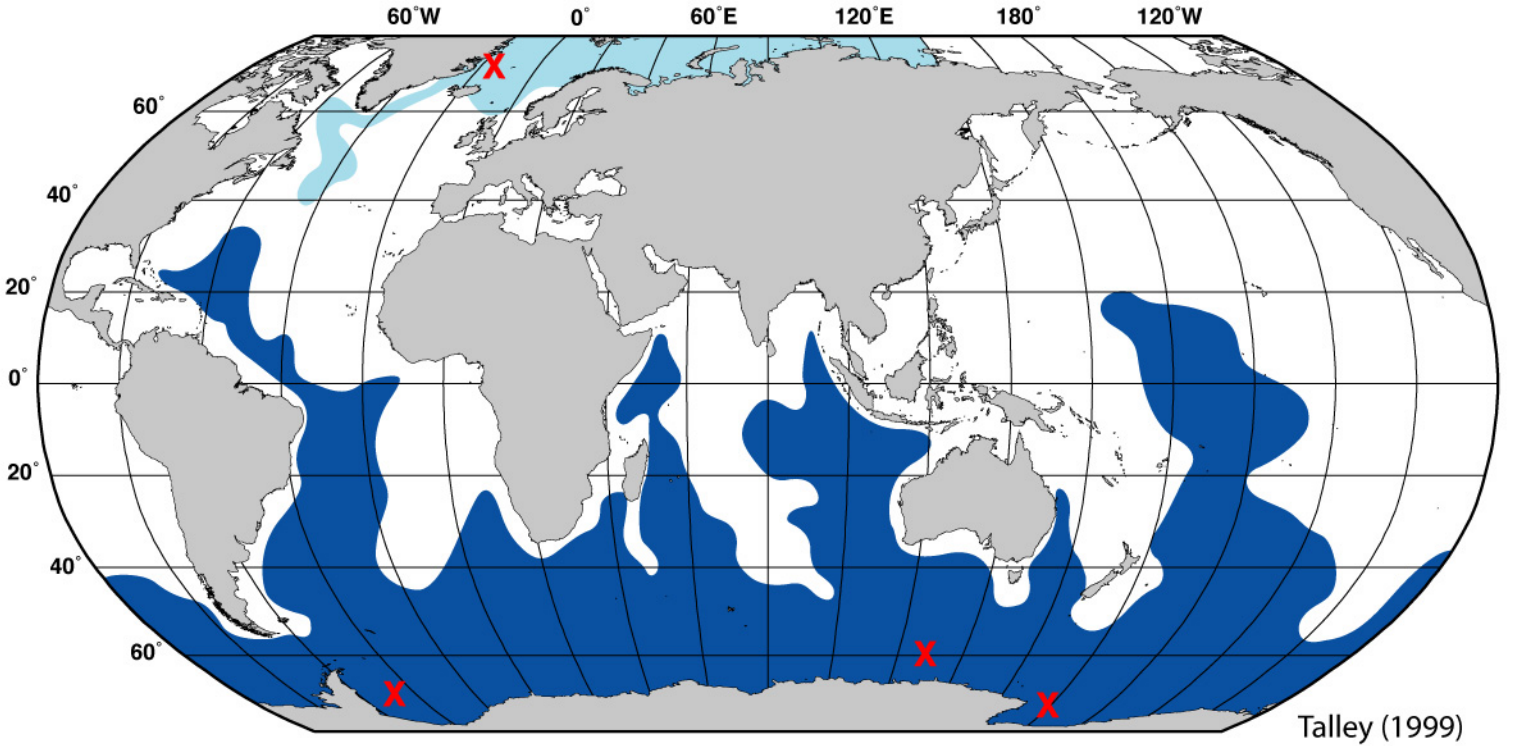
60˚W
0˚
60˚E
120˚E
180˚
120˚W
60˚
40˚
20˚
0˚
20˚
40˚
60˚
Talley (1999)

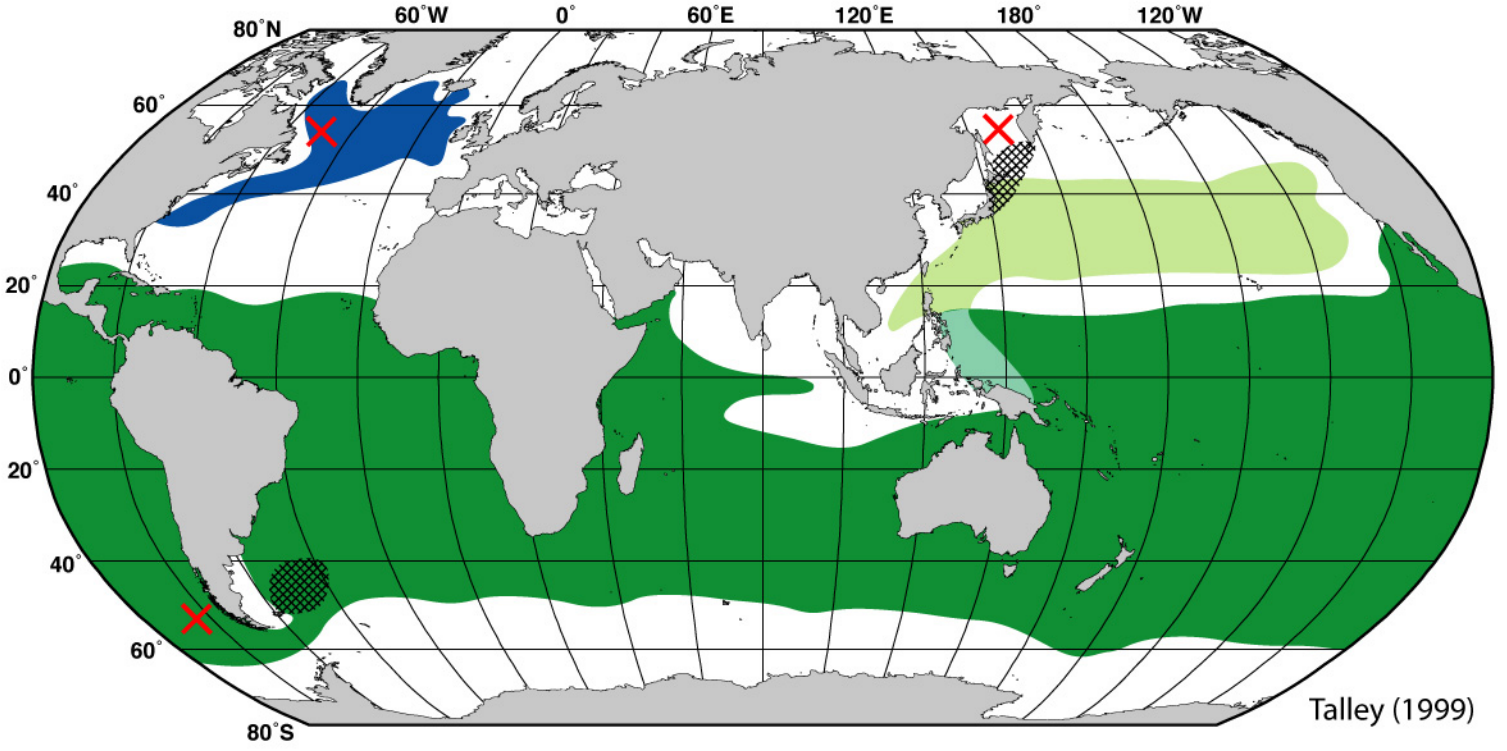
80˚N
60˚W
0˚
60˚E
120˚E
180˚
120˚W
60˚
40˚
20˚
0˚
20˚
40˚
60˚
80˚S
Talley (1999)

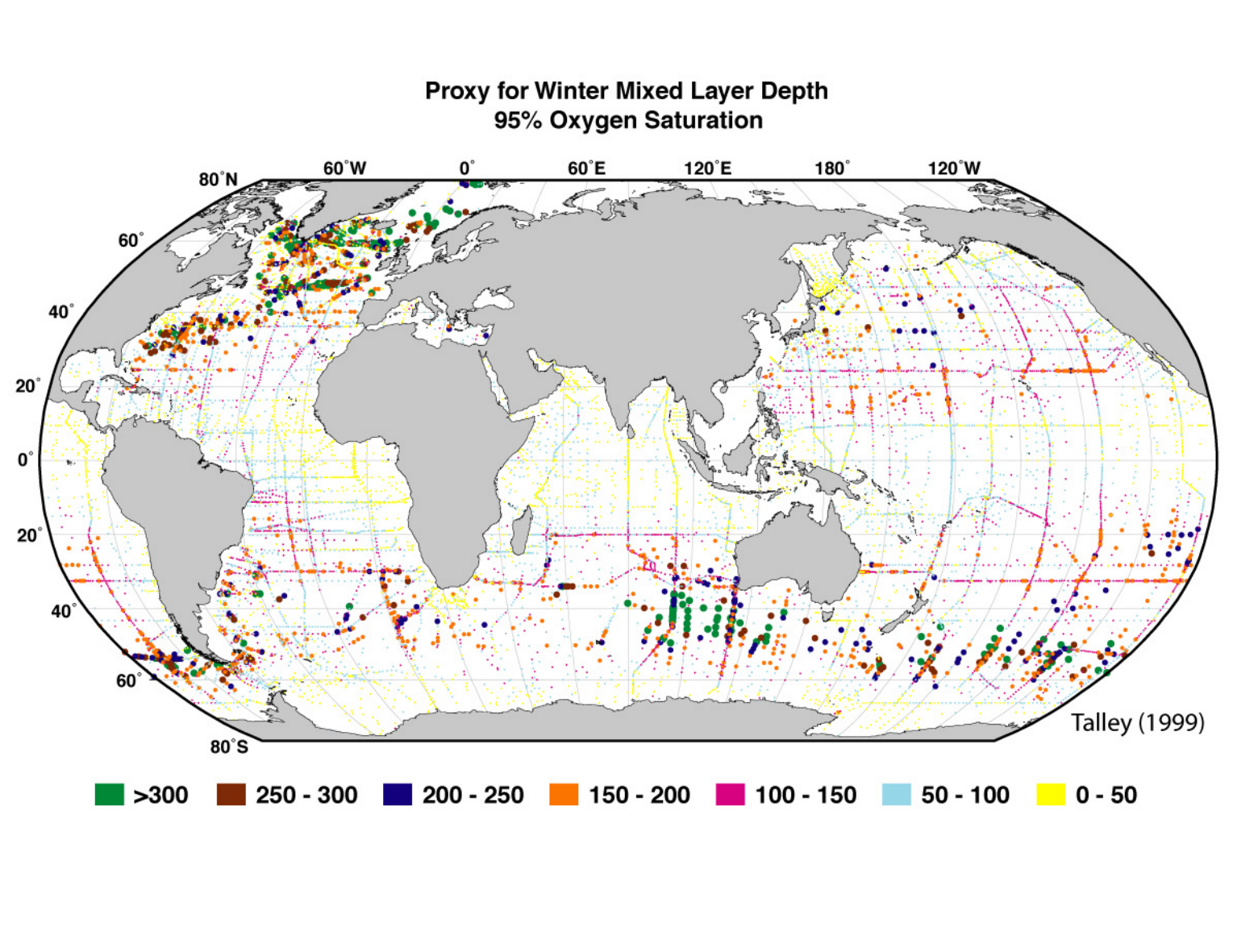
Proxy for Winter Mixed Layer Depth
95% Oxygen Saturation
80°N
60°W
0°
60°E
120°E
180°
120°W
60°
40°
20°
0°
20°
40°
60°
80°S
Talley (1999)
>300
250 - 300
200 - 250
150 - 200
100 - 150
50 - 100
0 - 50